

Diffusion as a possible mechanism controlling
the production of superheavy nuclei
in cold fusion reactions

T. Cap, BP1

M. Kowal, BP2

K. Siwek-Wilczyńska, ZFJ, FUW



NATIONAL
CENTRE
FOR NUCLEAR
RESEARCH
ŚWIERK

Periodic Table of the Elements

1 1IA 1A

2 IIA 2A

13 IIIA 3A

14 IVA 4A

15 VA 5A

16 VIA 6A

17 VIIA 7A

18 VIIIA 8A

1 H Hydrogen 1.008

2 He Helium 4.003

3 Li Lithium 6.941

4 Be Beryllium 9.012

5 B Boron 10.811

6 C Carbon 12.011

7 N Nitrogen 14.007

8 O Oxygen 15.999

9 F Fluorine 18.998

10 Ne Neon 20.180

11 Na Sodium 22.99

12 Mg Magnesium 24.305

13 Al Aluminum 26.982

14 Si Silicon 28.086

15 P Phosphorus 30.974

16 S Sulfur 32.066

17 Cl Chlorine 35.453

18 Ar Argon 39.948

19 K Potassium 39.098

20 Ca Calcium 40.078

21 Sc Scandium 44.956

22 Ti Titanium 47.867

23 V Vanadium 50.942

24 Cr Chromium 51.996

25 Mn Manganese 54.938

26 Fe Iron 55.845

27 Co Cobalt 58.933

28 Ni Nickel 58.693

29 Cu Copper 63.546

30 Zn Zinc 65.38

31 Ga Gallium 69.723

32 Ge Germanium 72.631

33 As Arsenic 74.922

34 Se Selenium 78.971

35 Br Bromine 79.904

36 Kr Krypton 83.789

37 Rb Rubidium 85.468

38 Sr Strontium 87.62

39 Y Yttrium 88.906

40 Zr Zirconium 91.224

41 Nb Niobium 92.906

42 Mo Molybdenum 95.95

43 Tc Technetium 98.907

44 Ru Ruthenium 101.07

45 Rh Rhodium 102.906

46 Pd Palladium 106.42

47 Ag Silver 107.868

48 Cd Cadmium 112.414

49 In Indium 114.818

50 Sn Tin 118.711

51 Sb Antimony 121.760

52 Te Tellurium 127.6

53 I Iodine 126.904

54 Xe Xenon 131.294

55 Cs Cesium 132.905

56 Ba Barium 137.328

57-71 Lanthanide Series

72 Hf Hafnium

73 Ta Tantalum

74 W Tungsten

75 Re Rhenium

76 Os Osmium

77 Ir Iridium

78 Pt Platinum

79 Au Gold

80 Hg Mercury

81 Tl Thallium

82 Pb Lead

83 Bi Bismuth

84 Po Polonium

85 At Astatine

86 Rn Radon

87 Fr Francium 223.020

88 Ra Radium 226.025

89-103 Actinide Series

104 Rf Rutherfordium [261]

105 Db Dubnium [262]

106 Sg Seaborgium [266]

107 Bh Bohrium [264]

108 Hs Hassium [269]

109 Mt Meitnerium [276]

110 Ds Darmstadtium [281]

111 Rg Roentgenium [280]

112 Cn Copernicium [285]

113 Nh Nihonium [286]

114 Fl Flerovium [289]

115 Mc Moscovium [288]

116 Lv Livermorium [293]

117 Ts Tennessine [294]

118 Og Oganesson [294]

57 La Lanthanum 138.905

58 Ce Cerium 140.116

59 Pr Praseodymium 140.908

60 Nd Neodymium 144.243

61 Pm Promethium 144.913

62 Sm Samarium 150.36

63 Eu Europium 151.964

64 Gd Gadolinium 157.25

65 Tb Terbium 158.925

66 Dy Dysprosium 162.500

67 Ho Holmium 164.930

68 Er Erbium 167.259

69 Tm Thulium 168.934

70 Yb Ytterbium 173.055

71 Lu Lutetium 174.967

89 Ac Actinium 227.028

90 Th Thorium 232.038

91 Pa Protactinium 231.036

92 U Uranium 238.029

93 Np Neptunium 237.048

94 Pu Plutonium 244.064

95 Am Americium 243.061

96 Cm Curium 247.070

97 Bk Berkelium 247.070

98 Cf Californium 251.080

99 Es Einsteinium [254]

100 Fm Fermium 257.095

101 Md Mendelevium 258.1

102 No Nobelium 259.101

103 Lr Lawrencium [262]

Alkali Metal

Alkaline Earth

Transition Metal

Basic Metal

Semimetal

Nonmetal

Halogen

Noble Gas

Lanthanide

Actinide

Superheavy elements
(Transactinides)

SHE = TAN ($Z \geq 104$)

15 elements discovered
in 50 years

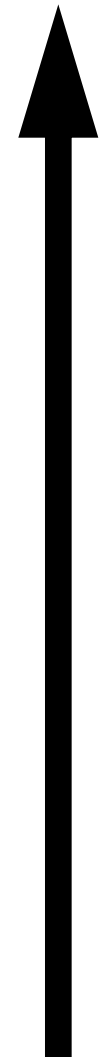
138 nuclides (SHN)

8th row: 119 (ongoing exp. at RIKEN), 120 (ongoing exp. at DUBNA)

SHN are synthesized in fusion reactions
or identified in decay chains of the fusion products

Projectile + Target \rightarrow SHN*

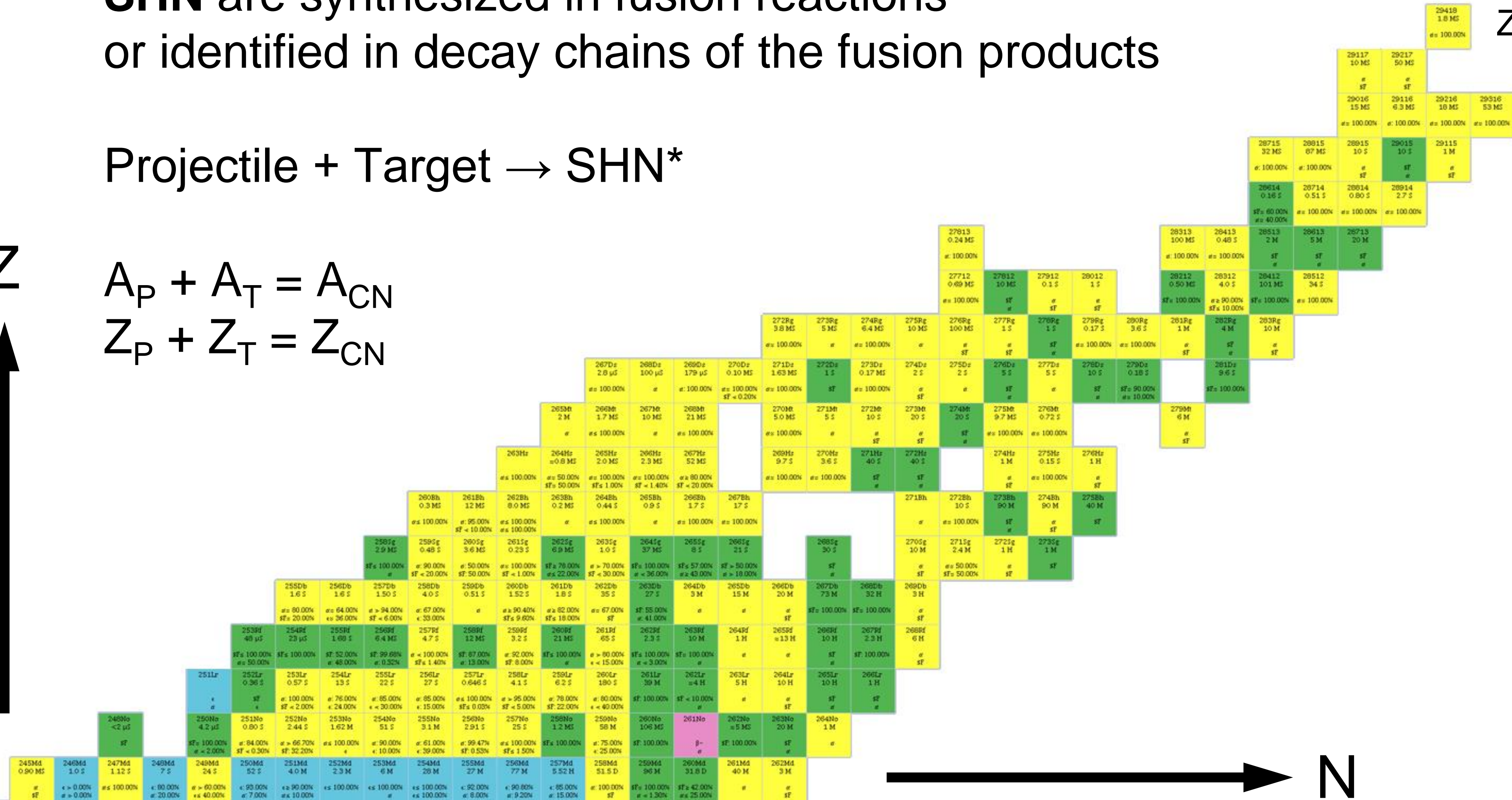
Z



$$A_P + A_T = A_{CN}$$

$$Z_P + Z_T = Z_{CN}$$

Z = 118



N



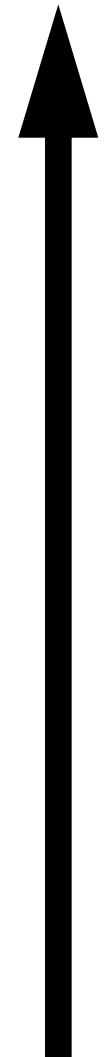
Cold Fusion Reactions



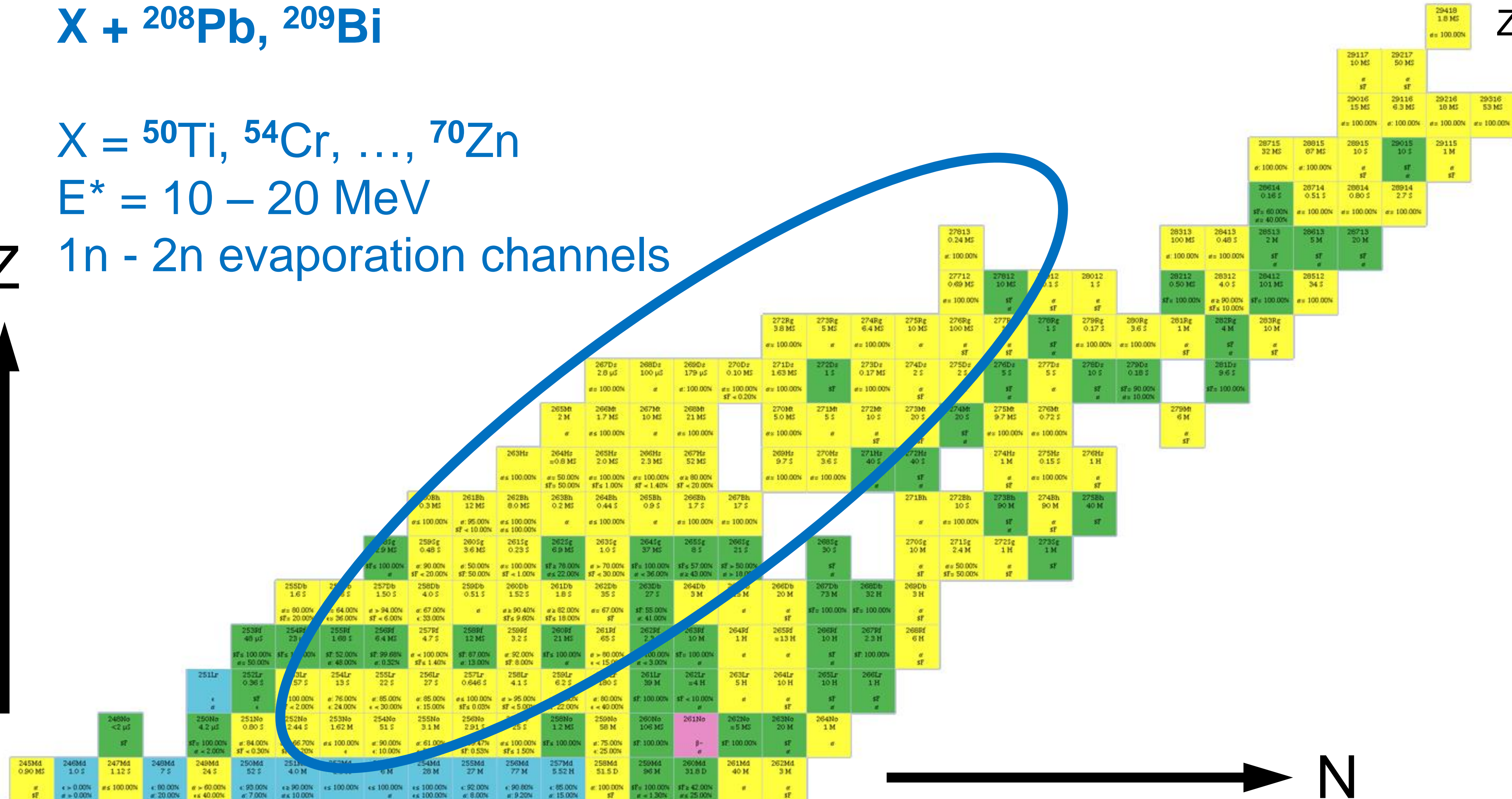
$$E^* = 10 - 20 \text{ MeV}$$

1n - 2n evaporation channels

Z



Z = 118



Hot Fusion Reactions

^{48}Ca + Actinide targets

Act. = ^{238}U , ^{244}Pu , ..., ^{249}Cf

$E^* = 30 - 40 \text{ MeV}$

3n - 4n evaporation channels

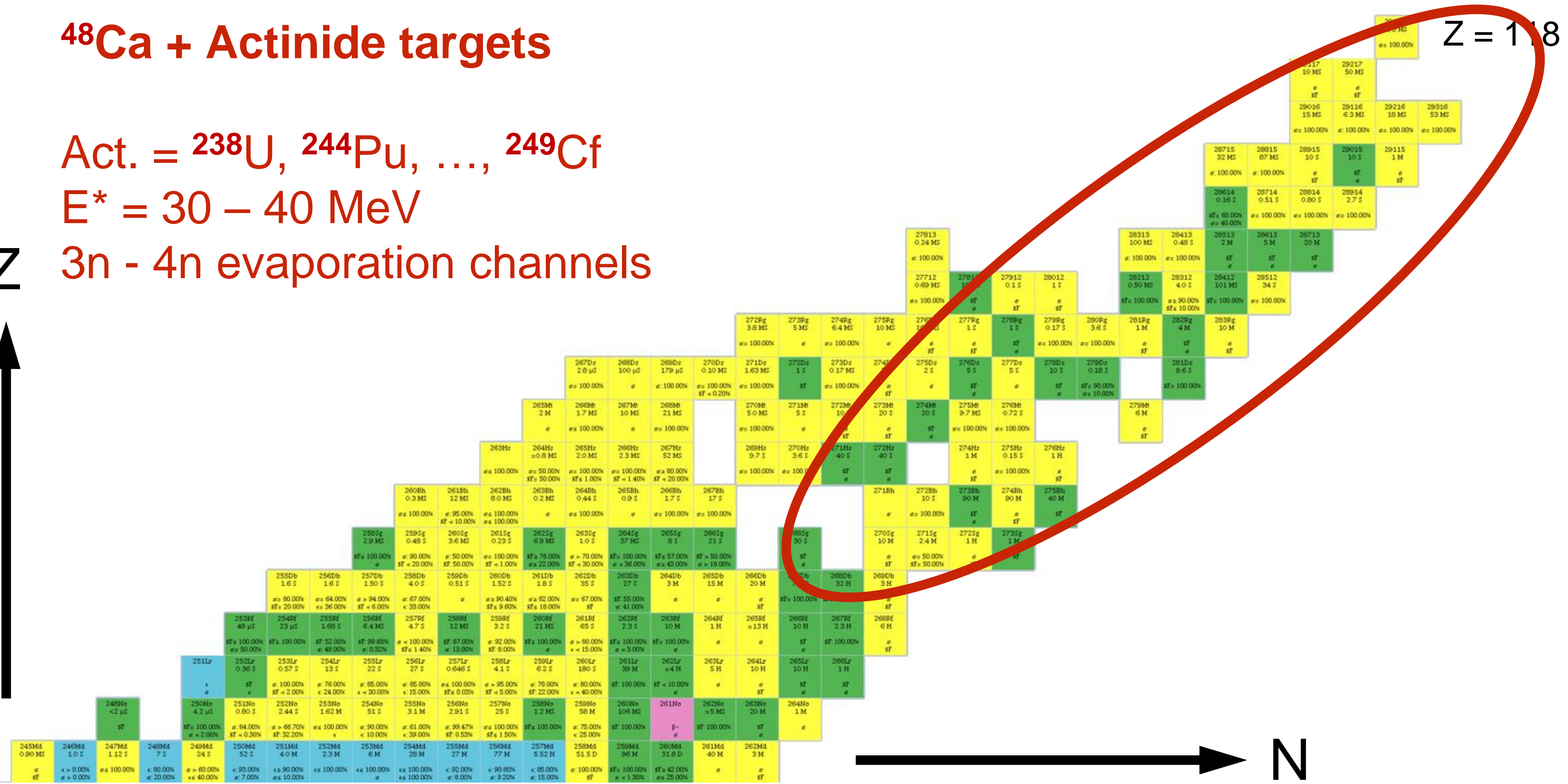
Z

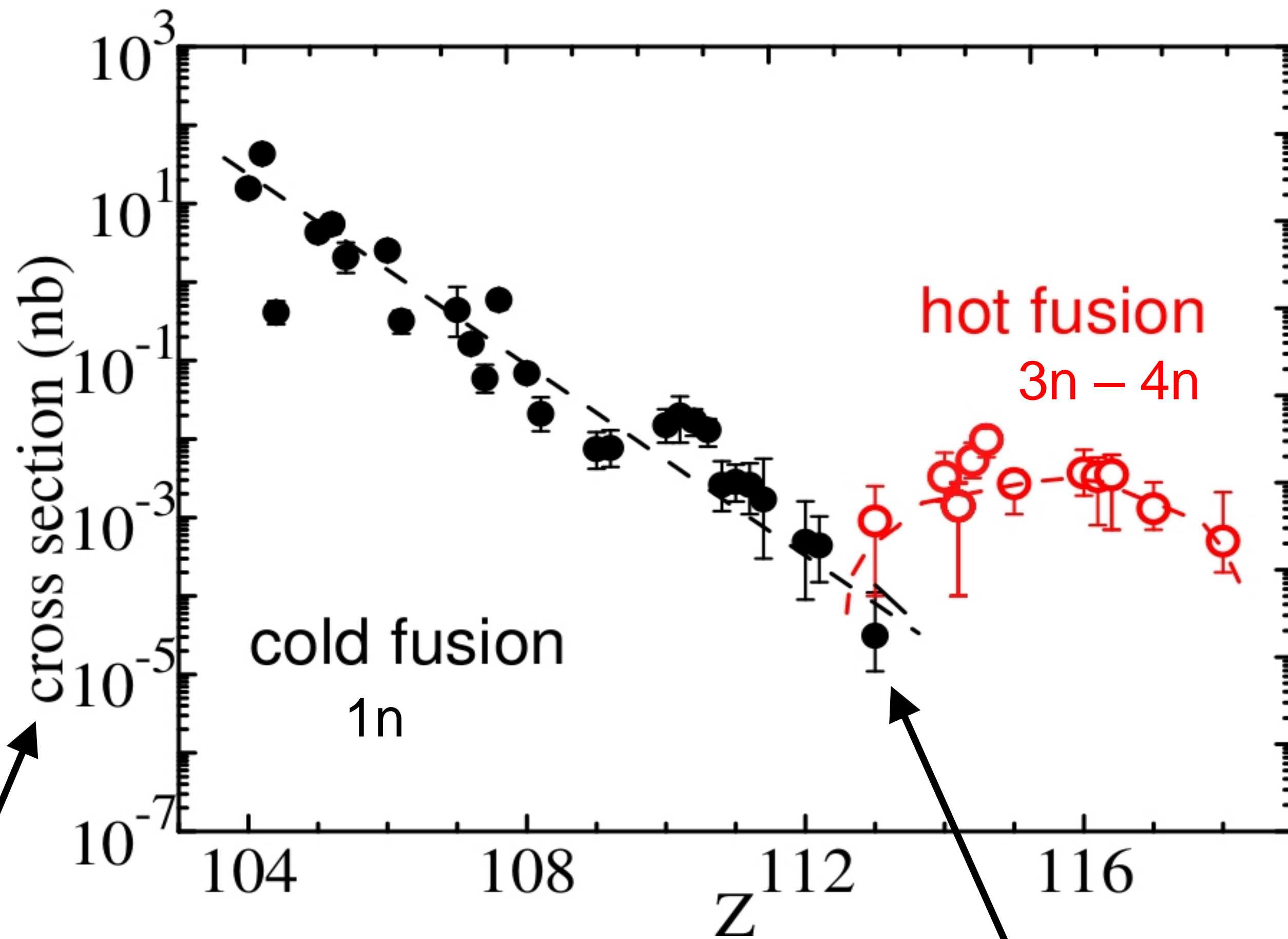


N



Z = 118





No heavier target than Cf (Z=98) is available

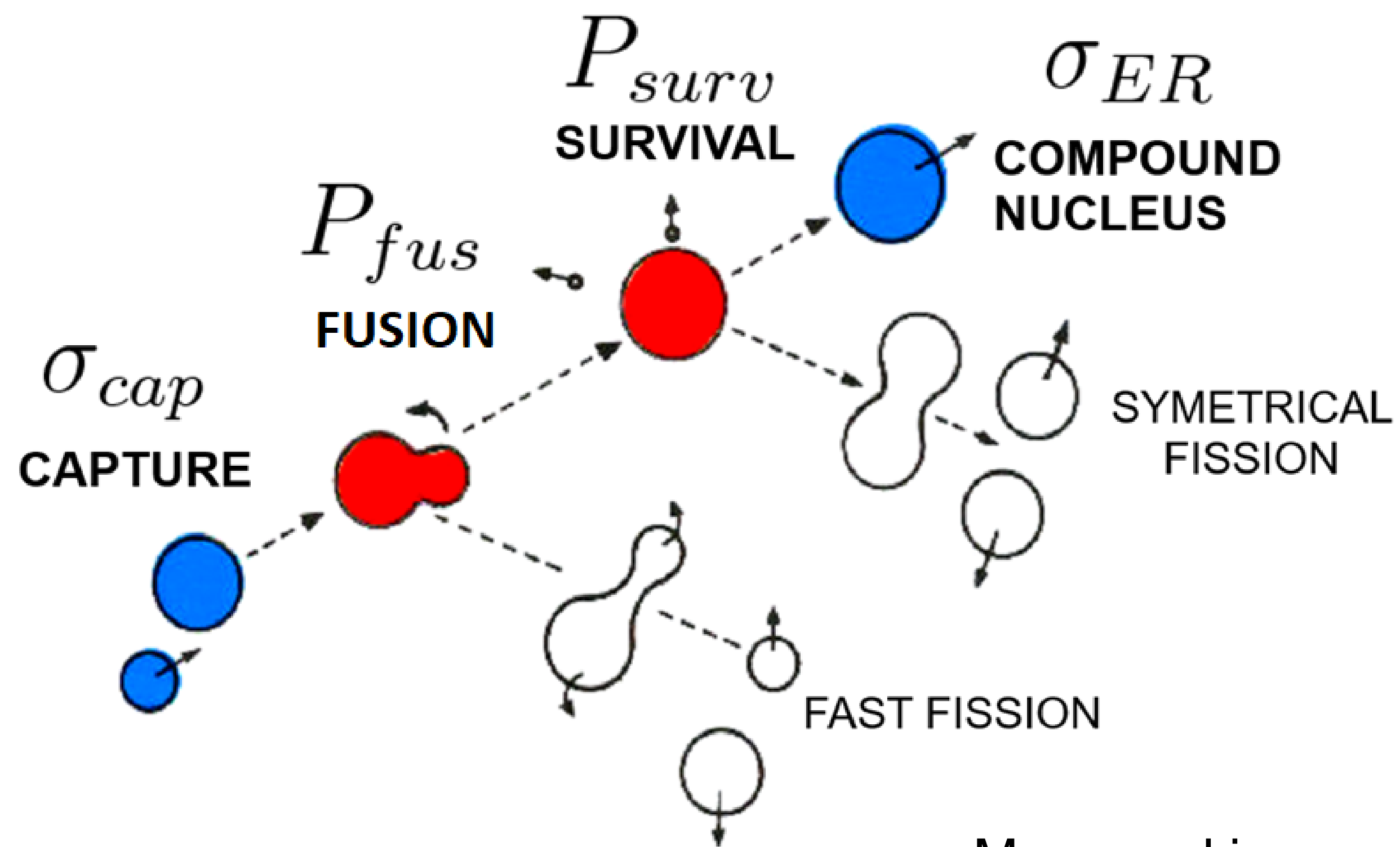
Es (Z=99) is too radioactive

Experiments with ^{51}V , ^{50}Ti , ^{54}Cr , and ^{56}Fe beams gave no results so far

Most of the experiments are focused on studying SHN properties and (recently) fusion reaction mechanisms.

Highest measured cross section for a given element

$Z=113$, 22 fb, only 3 atoms in 576 days of irradiation



FBD (fusion-by-diffusion)

Synthesis of SHN can be described as a 3 step process:

$$\sigma_{ER} = \sigma_{cap} P_{fus} P_{surv}$$

Not measured directly
Difficult to calculate

Well established theory and formulas
 $P_{surv} \ll 1$

Smoluchowski
Diffusion
equation

masses, fission
barriers, deformations
from Warsaw
Micro-Macro model

Measured in experiments, can be calculated using various models

Diffused barrier formula
(Gaussian distribution around mean entrance channel barrier B_0)

W. J. Świątecki, K. Siwek-Wilczyńska, J. Wilczyński, PRC 2005

T. Cap et al., PRC 2011

K. Siwek-Wilczyńska et al. PRC 2012

T. Cap et al., PRC 2013

K. Siwek-Wilczyńska et al. PRC 2019



Contents lists available at [ScienceDirect](https://www.sciencedirect.com)

Atomic Data and Nuclear Data Tables

journal homepage: www.elsevier.com/locate/adt



Properties of heaviest nuclei with $98 \leq Z \leq 126$ and $134 \leq N \leq 192$

P. Jachimowicz^a, M. Kowal^{b,*}, J. Skalski^b

^a Institute of Physics, University of Zielona Góra, Szafrana 4a, 65-516 Zielona Góra, Poland

^b National Centre for Nuclear Research, Pasteura 7, 02-093 Warsaw, Poland



Ground-state and saddle-point shapes and masses for 1305 heavy and superheavy nuclei including odd-A and odd–odd systems. Static fission barrier heights, one- and two-nucleon separation energies, and $Q\alpha$ values.

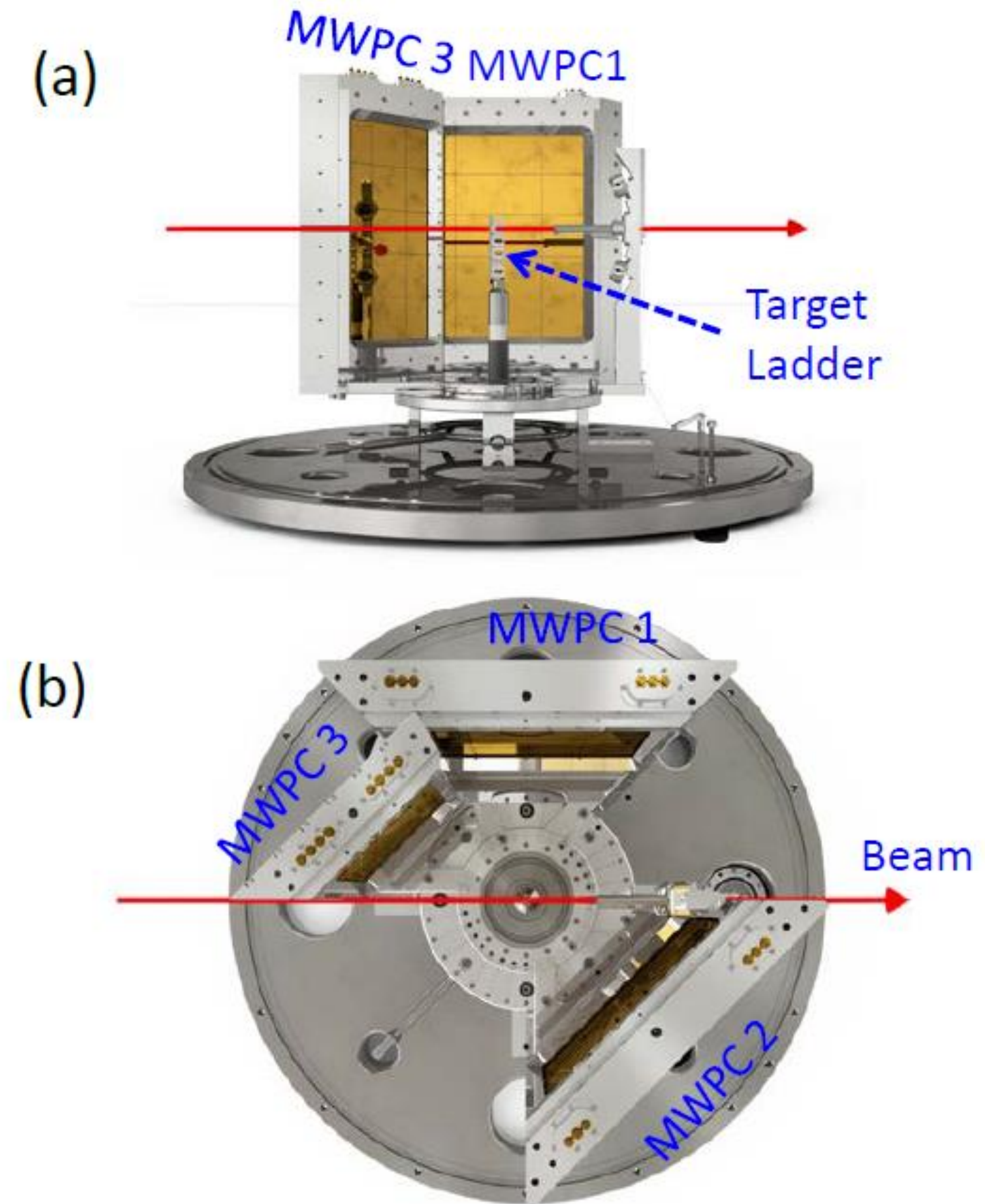
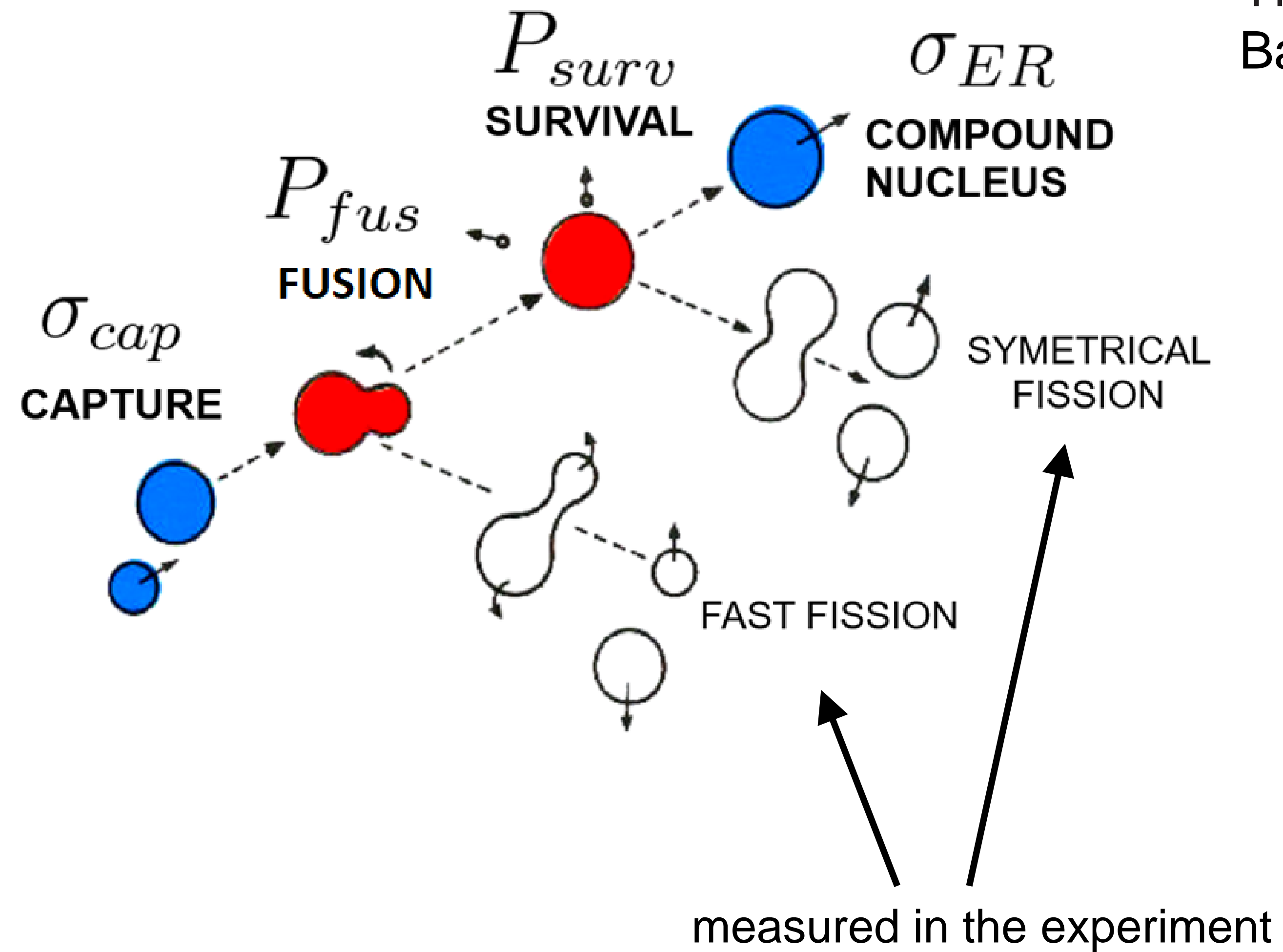
Microscopic–macroscopic method with the deformed Woods–Saxon single-particle potential and the Yukawa-plus-exponential macroscopic energy taken as the smooth part.

Ground-state shapes and energies are found by the minimization over **seven axially-symmetric deformations**. A search for saddle-points was performed by using the "imaginary water flow" method in three consecutive stages, using five- (for nonaxial shapes) and seven-dimensional (for reflection-asymmetric shapes) deformation spaces.

Good agreement with the experimental data for actinides.

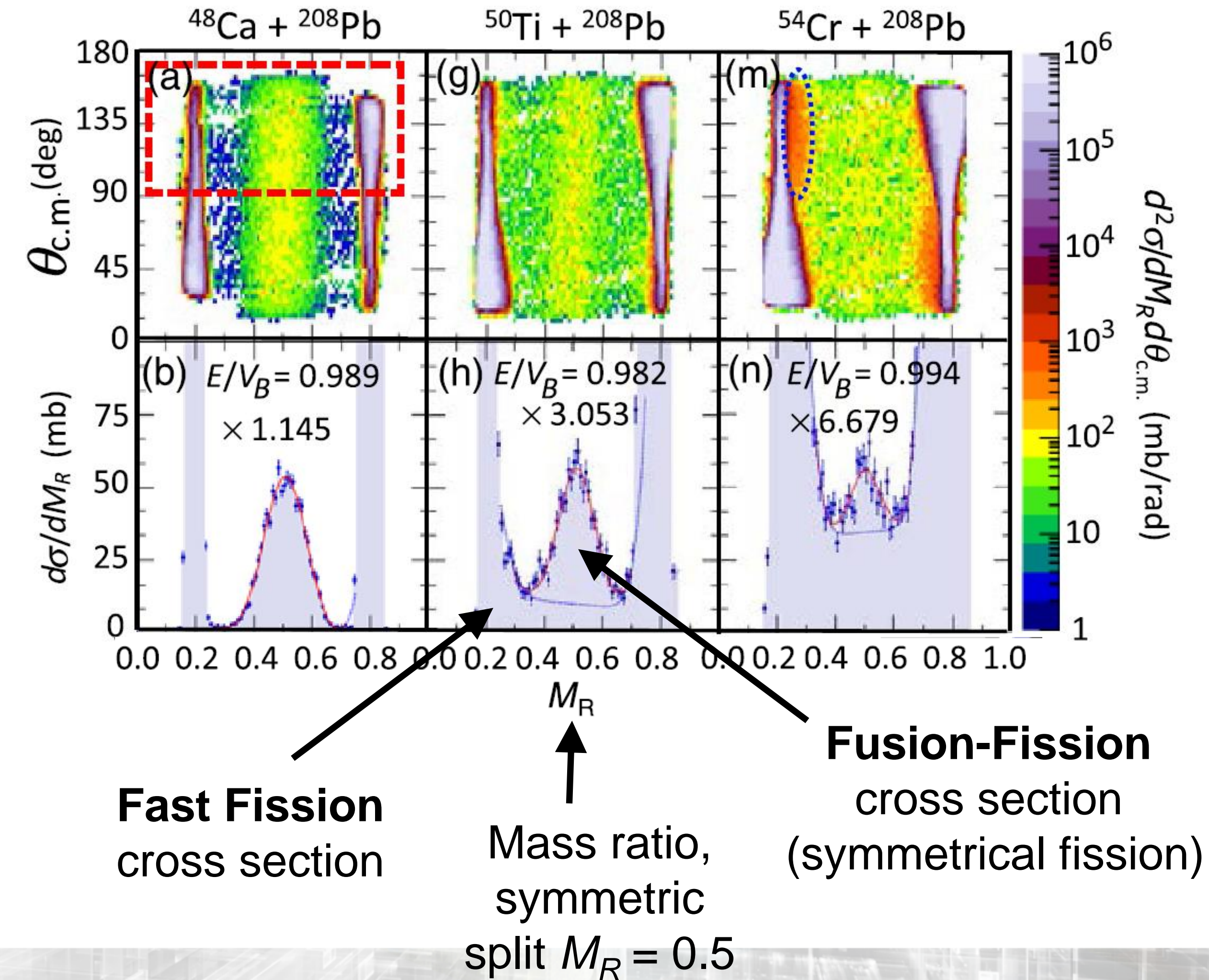
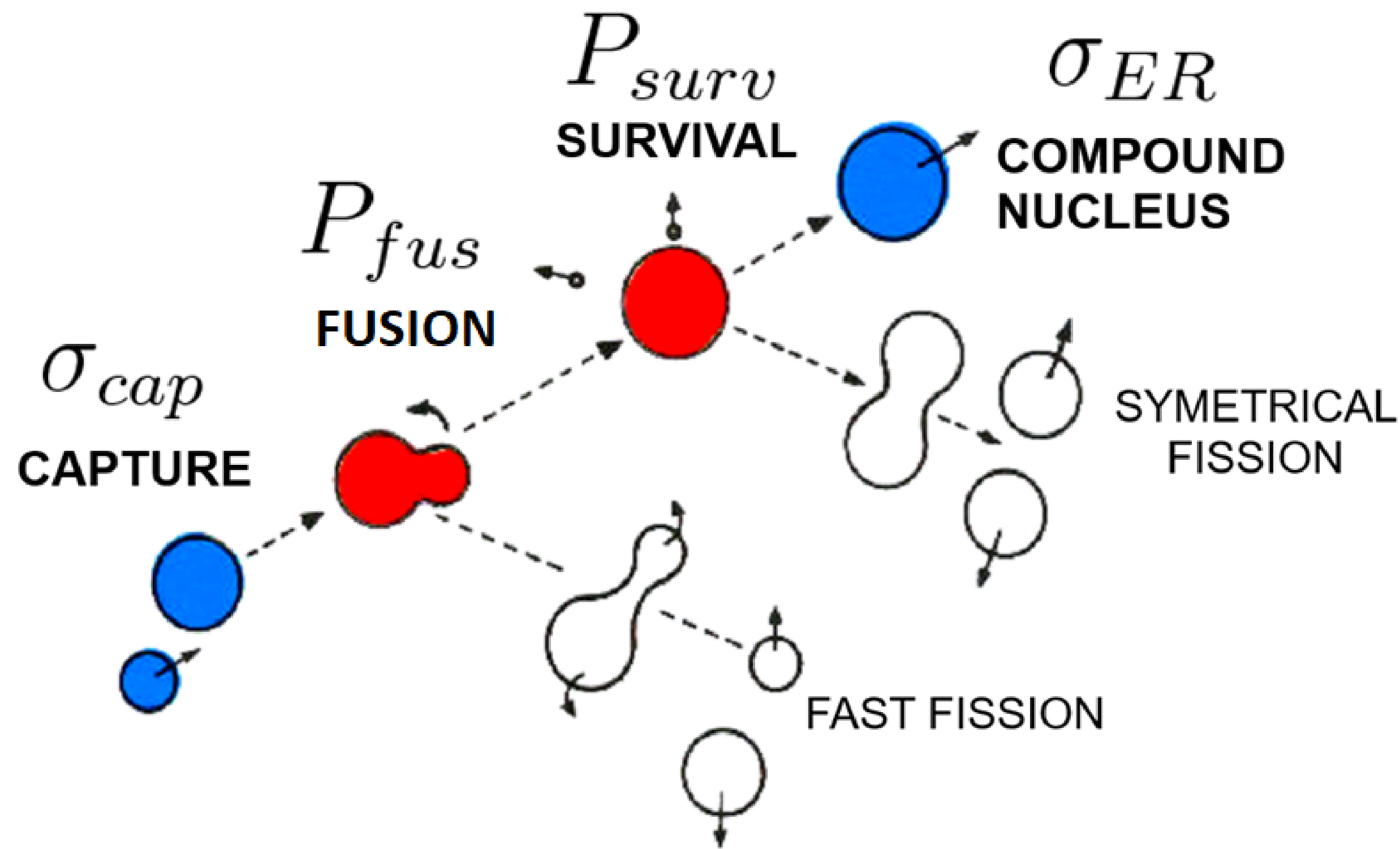
Mechanisms Suppressing Superheavy Element Yields in Cold Fusion Reactions

Banerjee et al., PRL 122, 232503 (2019)



Mechanisms Suppressing Superheavy Element Yields in Cold Fusion Reactions

Banerjee et al., PRL 122, 232503 (2019)

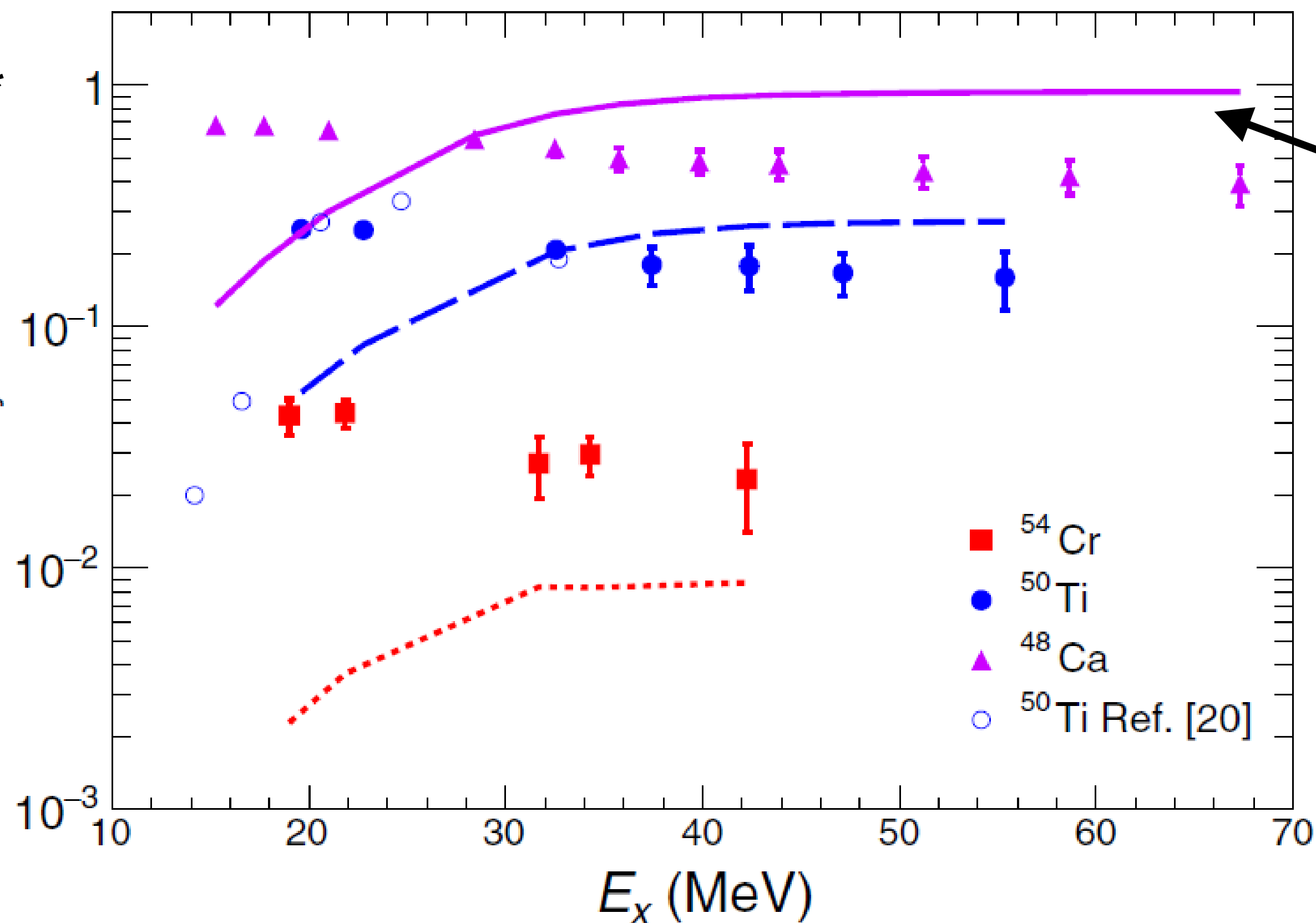


P_{fus} can be experimentally estimated:

$$P_{sym} = \frac{\text{Fusion-Fission cross section}}{\text{Capture cross section}}$$

Banerjee et al., PRL 122, 232503 (2019)

Reactions:



P_{sym}

Upper limit for Fusion Probability

E_x (MeV)

Excitation energy

Diffusion model calculations by V. Zagrebaev and W. Greiner PRC 78, 034610 (2008).

The experimental trend is different than the model predictions for all 3 reactions.

The conclusion was that diffusion is not the main mechanism responsible for the synthesis of SHN.

Questions:

Can the diffusion approach (FBD) describe the experimental results?

What is the fusion mechanism?

Fusion process on the Potential Energy Surface (PES)

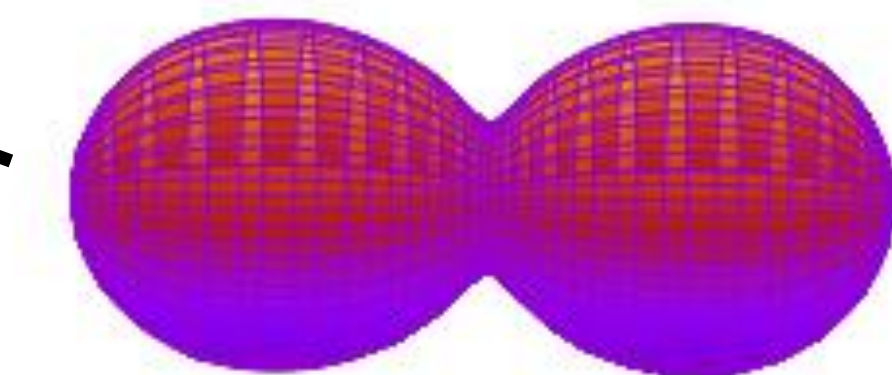
$$M(A,Z) = (A-Z)m_n + Zm_p + \text{Binding Energy}$$

Map for ^{256}No ($Z=102$)

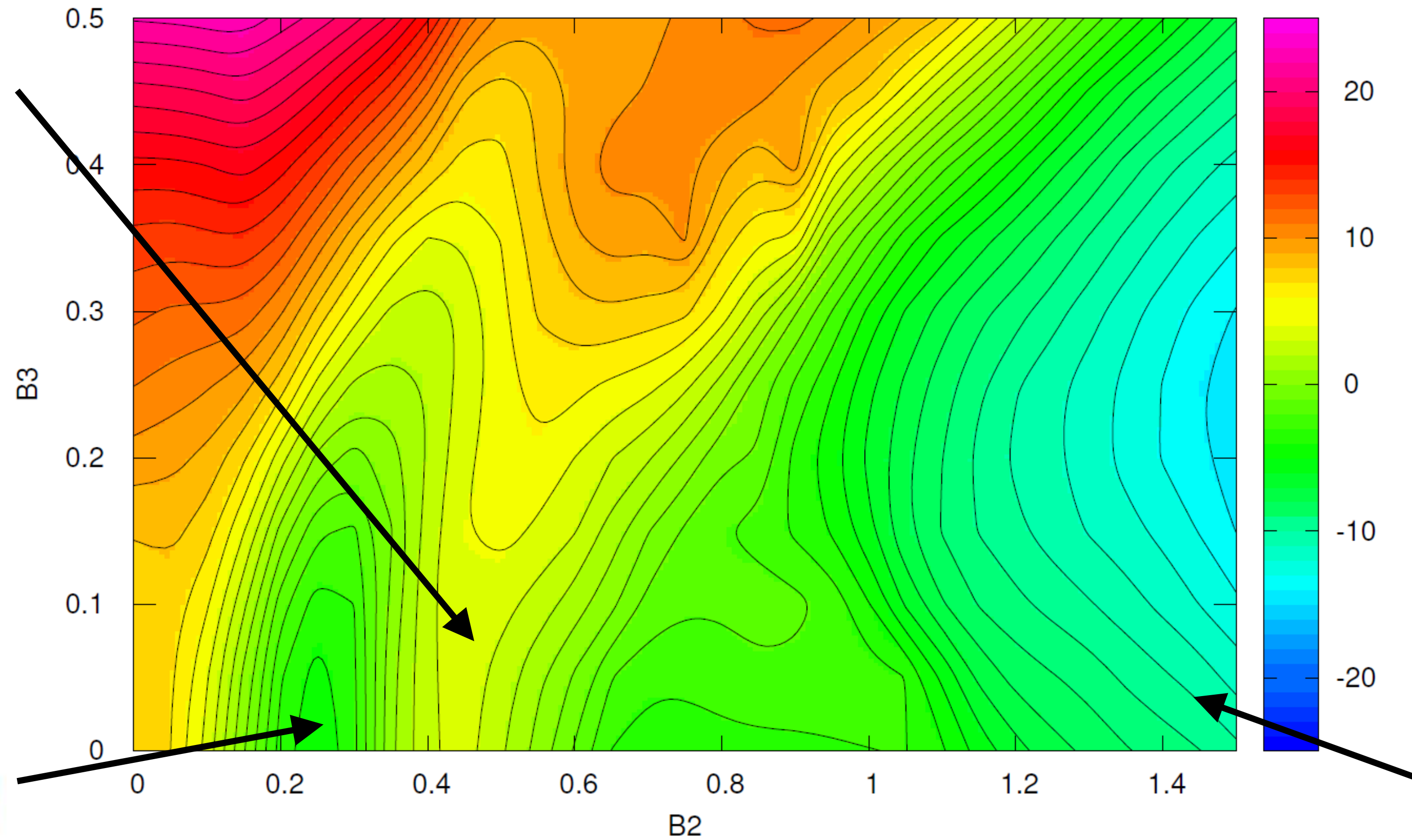
Based on
P. Jachimowicz, M. Kowal
and J. Skalski
ADNDT 138, 101393 (2021)

Calculations done by
Aleksander Augustyn in CIŚ

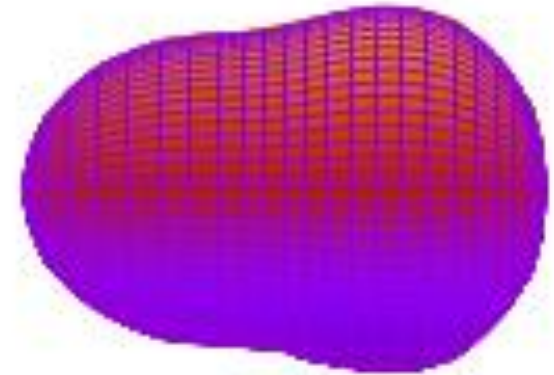
3D representation
of 8D space (200M point)



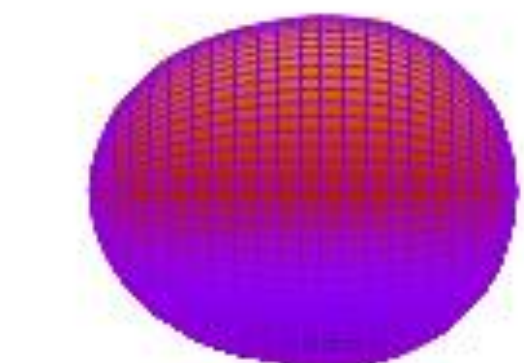
Scission point → Fission



Fission saddle point



$\beta_3 \approx$ asymmetry



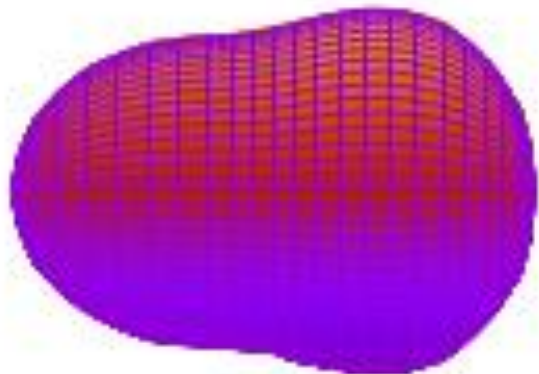
Ground state

$\beta_2 \approx$ elongation

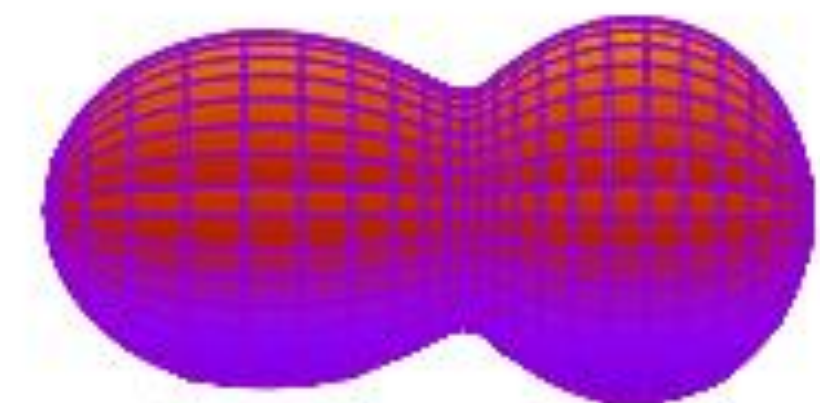
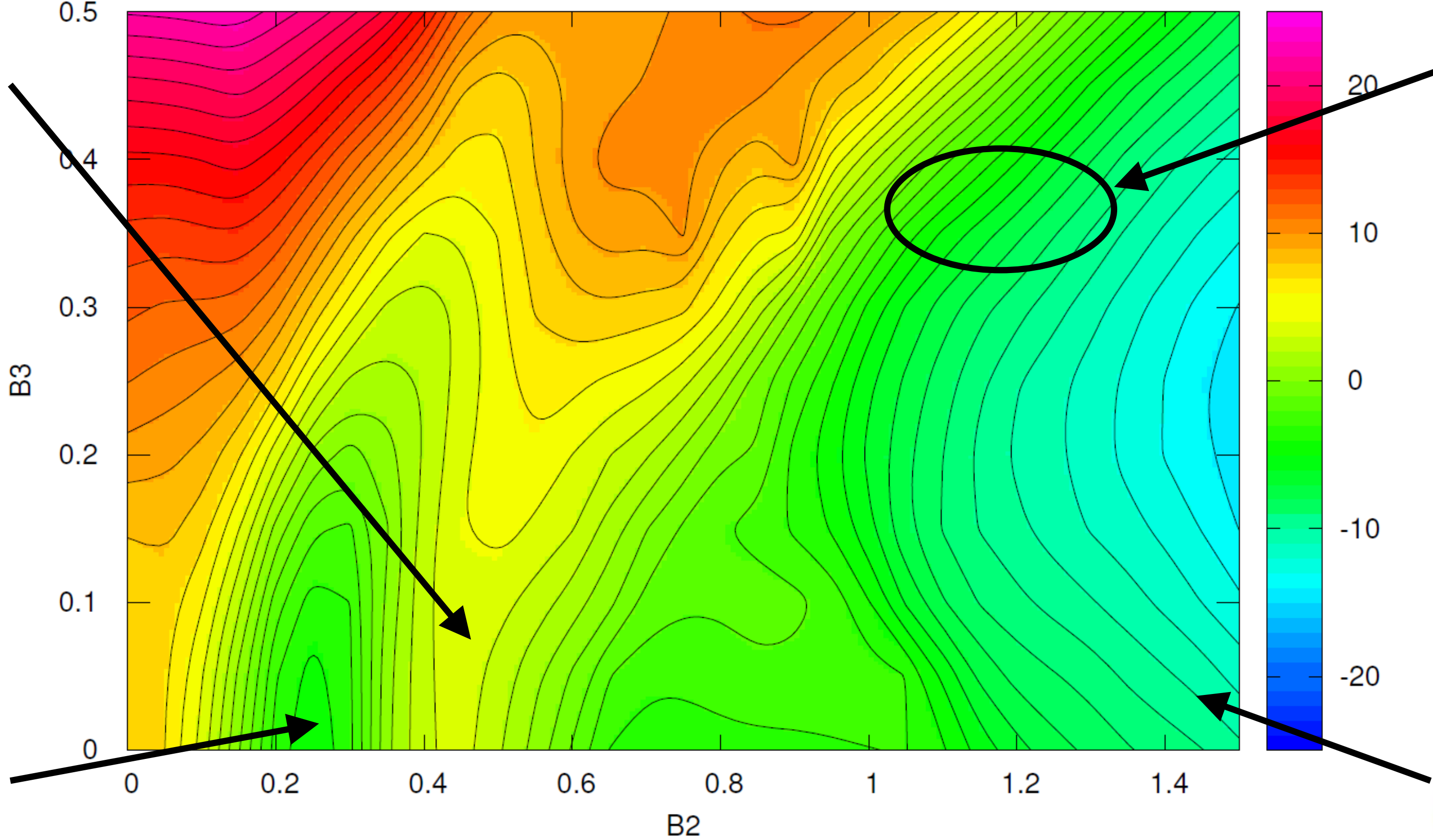
Fusion process on the Potential Energy Surface (PES)

$$M(A,Z) = (A-Z)m_n + Zm_p + \text{Binding Energy}$$

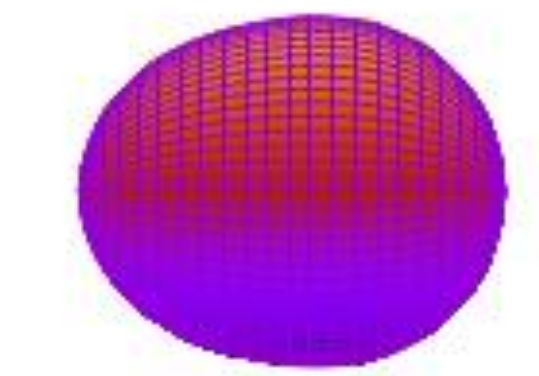
Fission saddle point



$\beta_3 \approx \text{asymmetry}$

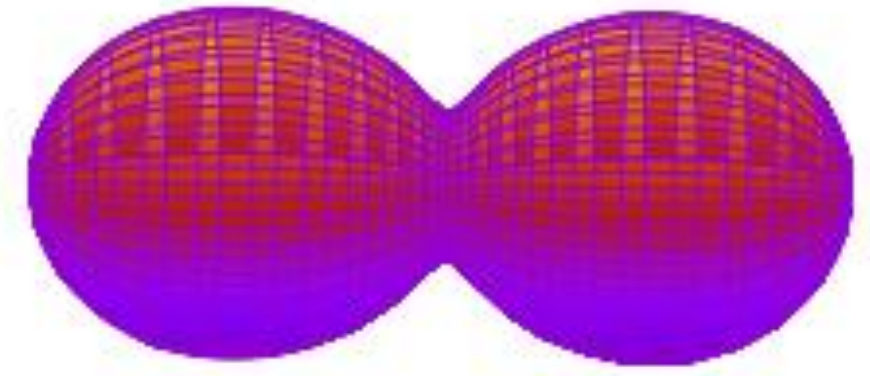


Starting point
(injection point)
 $^{48}\text{Ca} + ^{208}\text{Pb} \rightarrow ^{256}\text{No}$



Ground state

$\beta_2 \approx \text{elongation}$

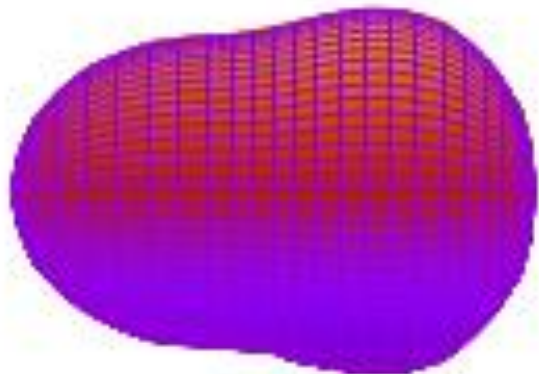


Scission point \rightarrow Fission

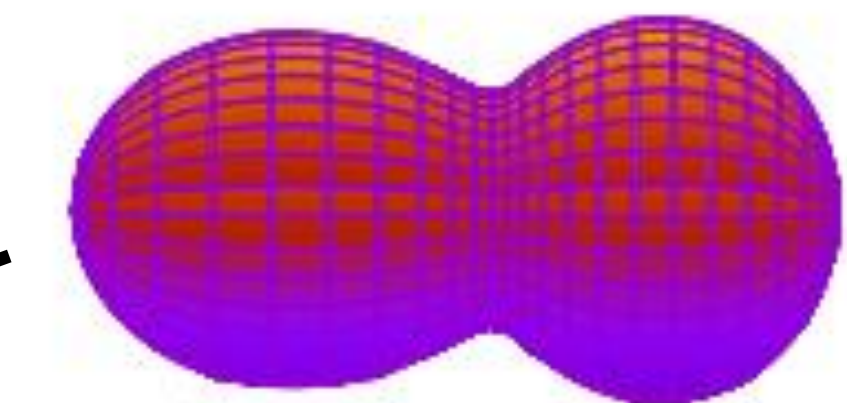
Fusion process on the Potential Energy Surface (PES)

$$M(A,Z) = (A-Z)m_n + Zm_p + \text{Binding Energy}$$

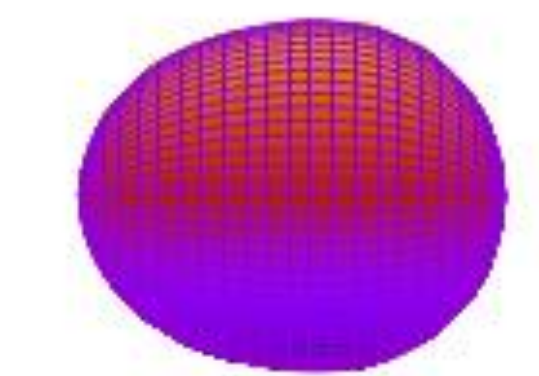
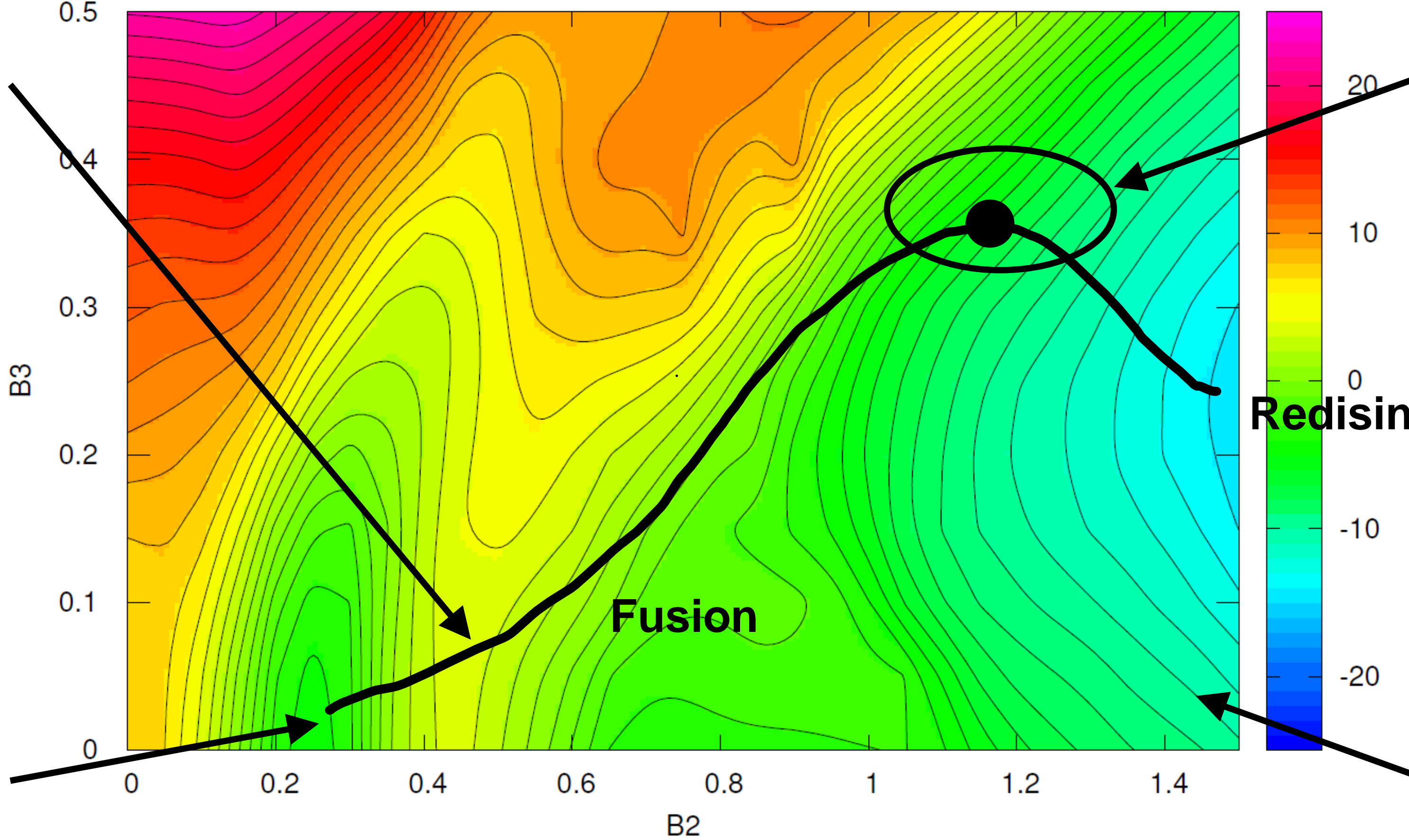
Fission saddle point



$\beta_3 \approx \text{asymmetry}$



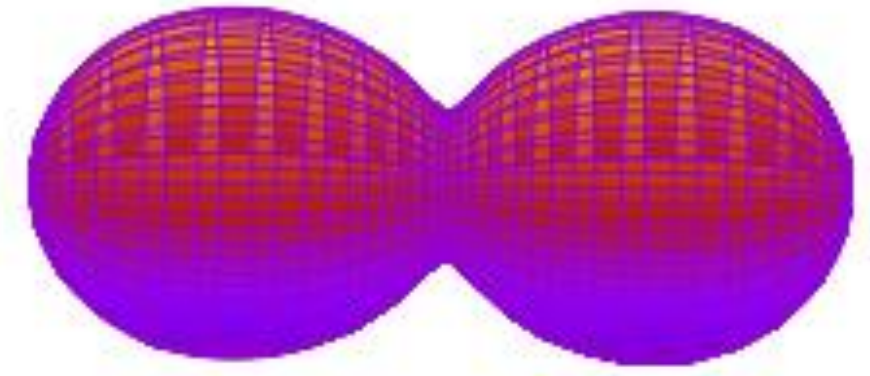
Starting point
(injection point)
 $^{48}\text{Ca} + ^{208}\text{Pb} \rightarrow ^{256}\text{No}$



Ground state

$\beta_2 \approx \text{elongation}$

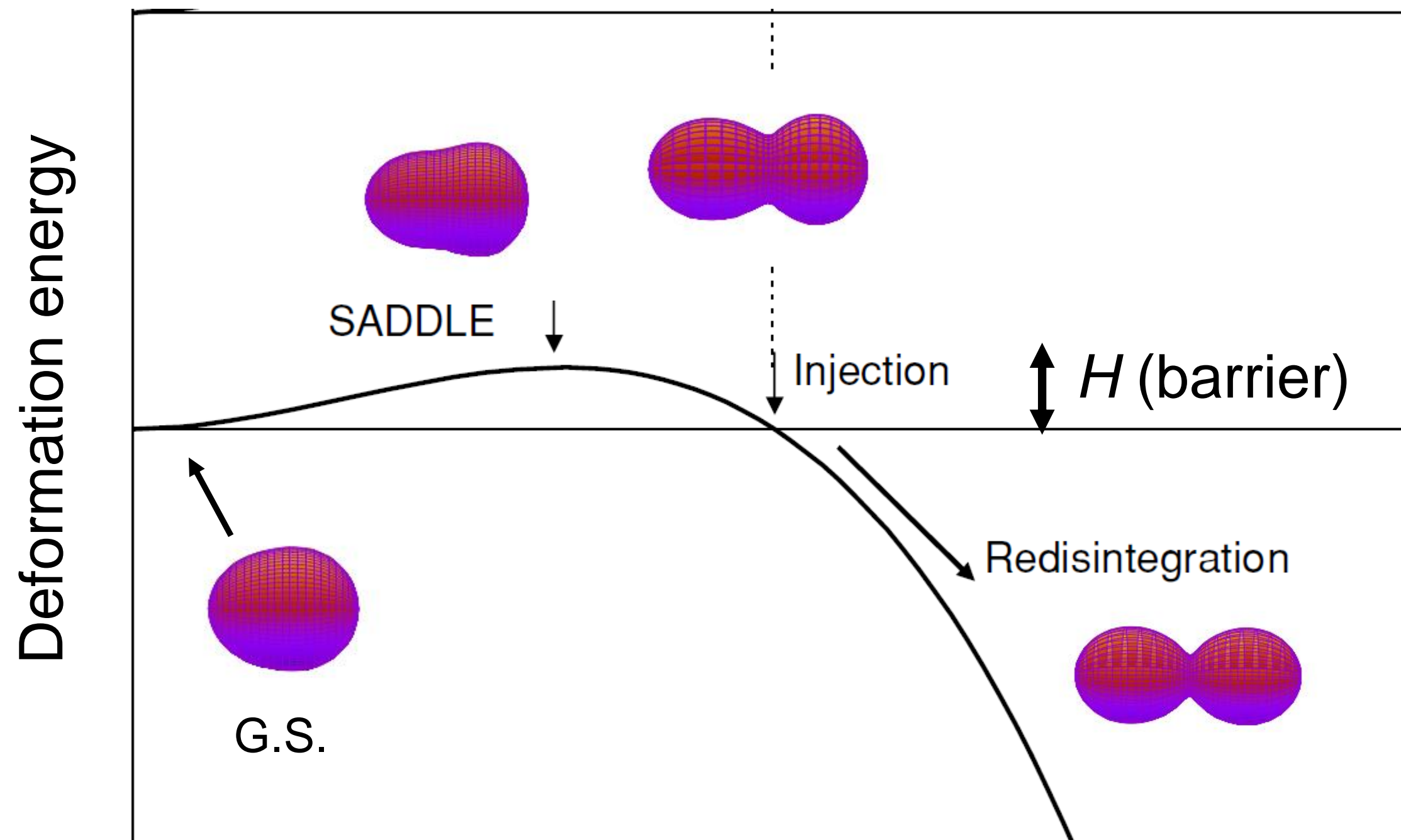
Redisintegration



Scission point \rightarrow Fission

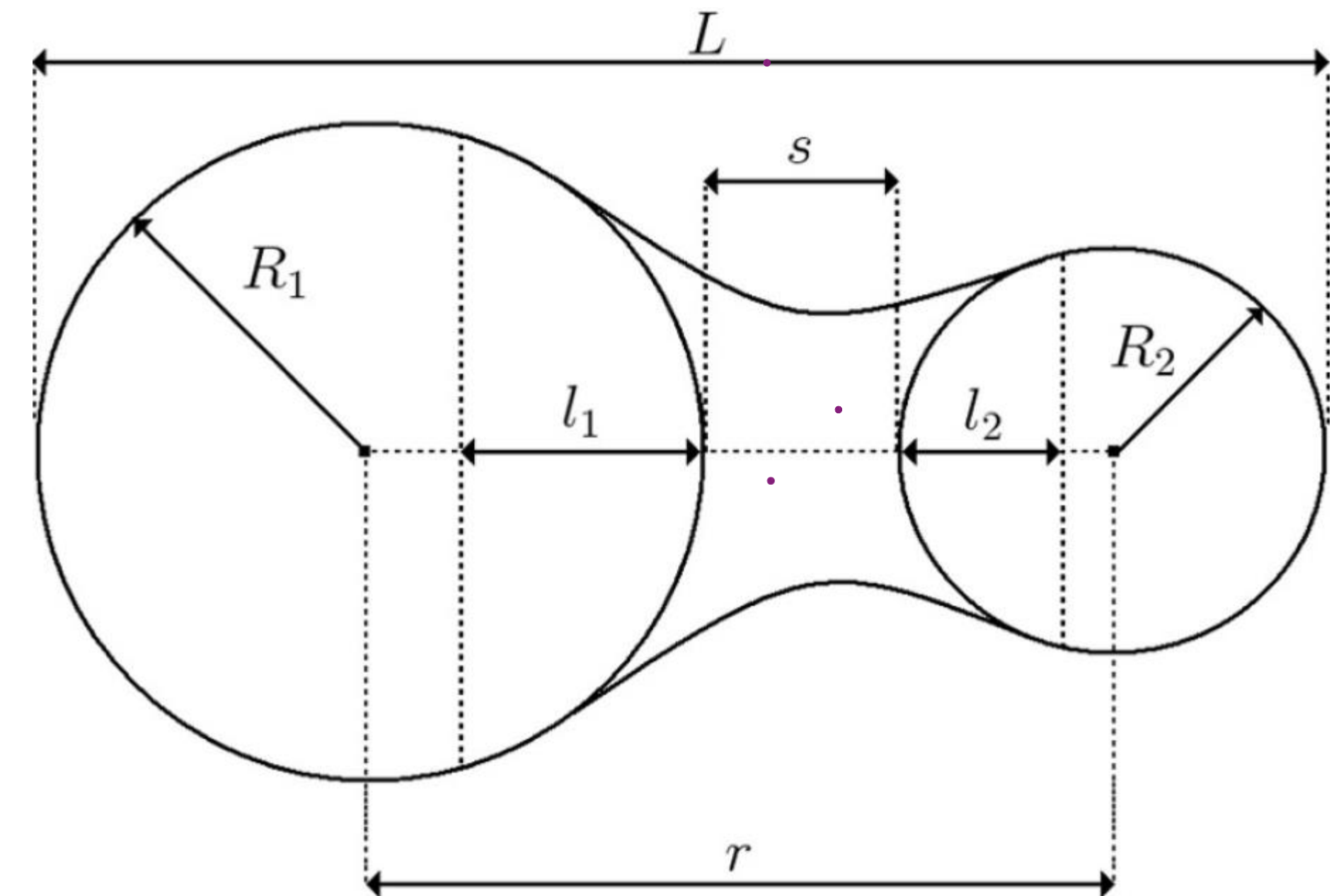
In the FBD model we use
1D motion approximation

The system must overcome an internal
barrier H to fuse.



L is the effective elongation (along the fusion path)

Macroscopic deformation energies are calculated using the parameterization of the nuclear shapes by two spheres joined smoothly by a third quadratic surface of revolution.

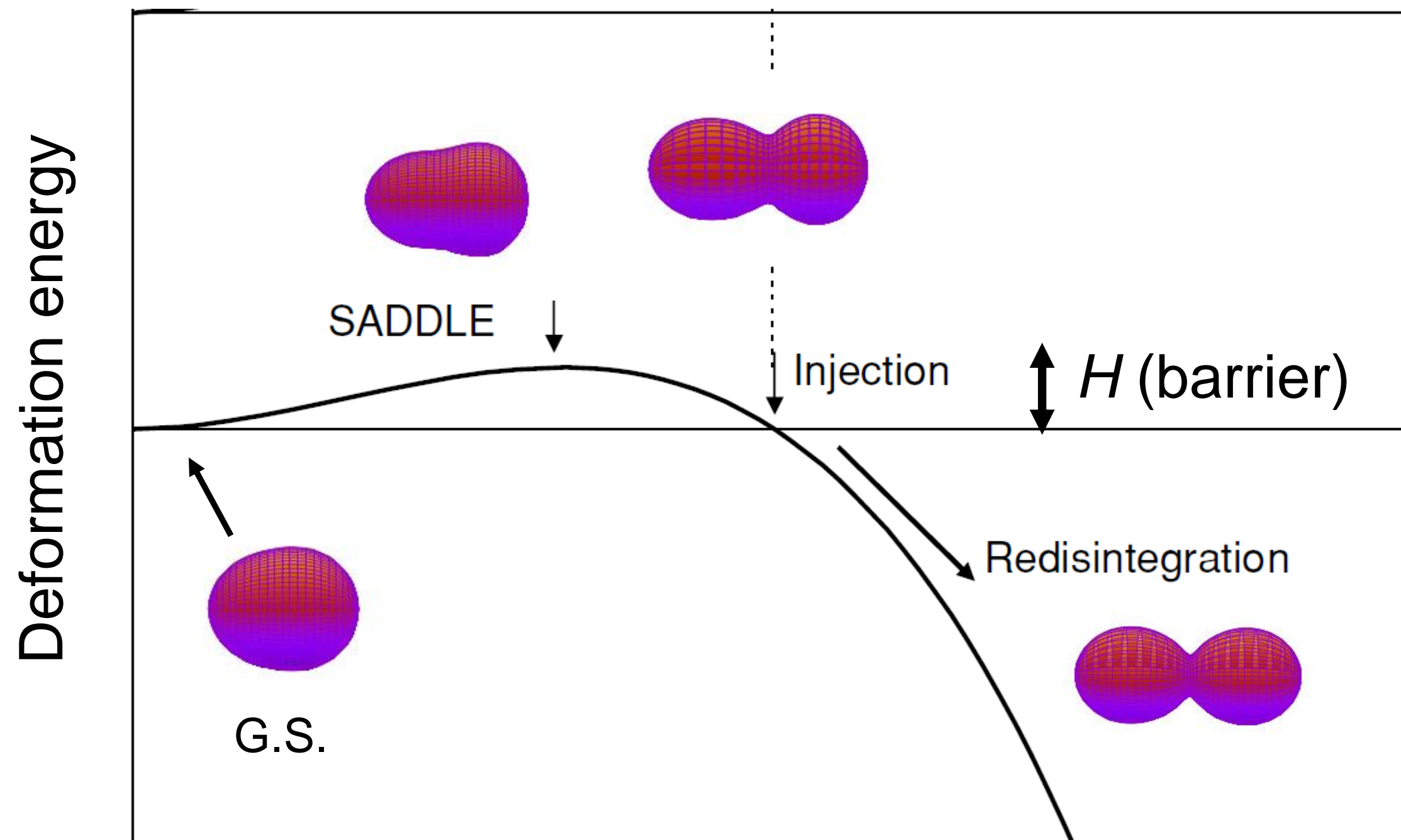


The distance between the nuclear surfaces of two colliding nuclei at the **injection** point, s_{inj} , is the only adjustable parameter of the model.

s_{inj} distance was parametrized by analyzing 27 cold fusion reactions.

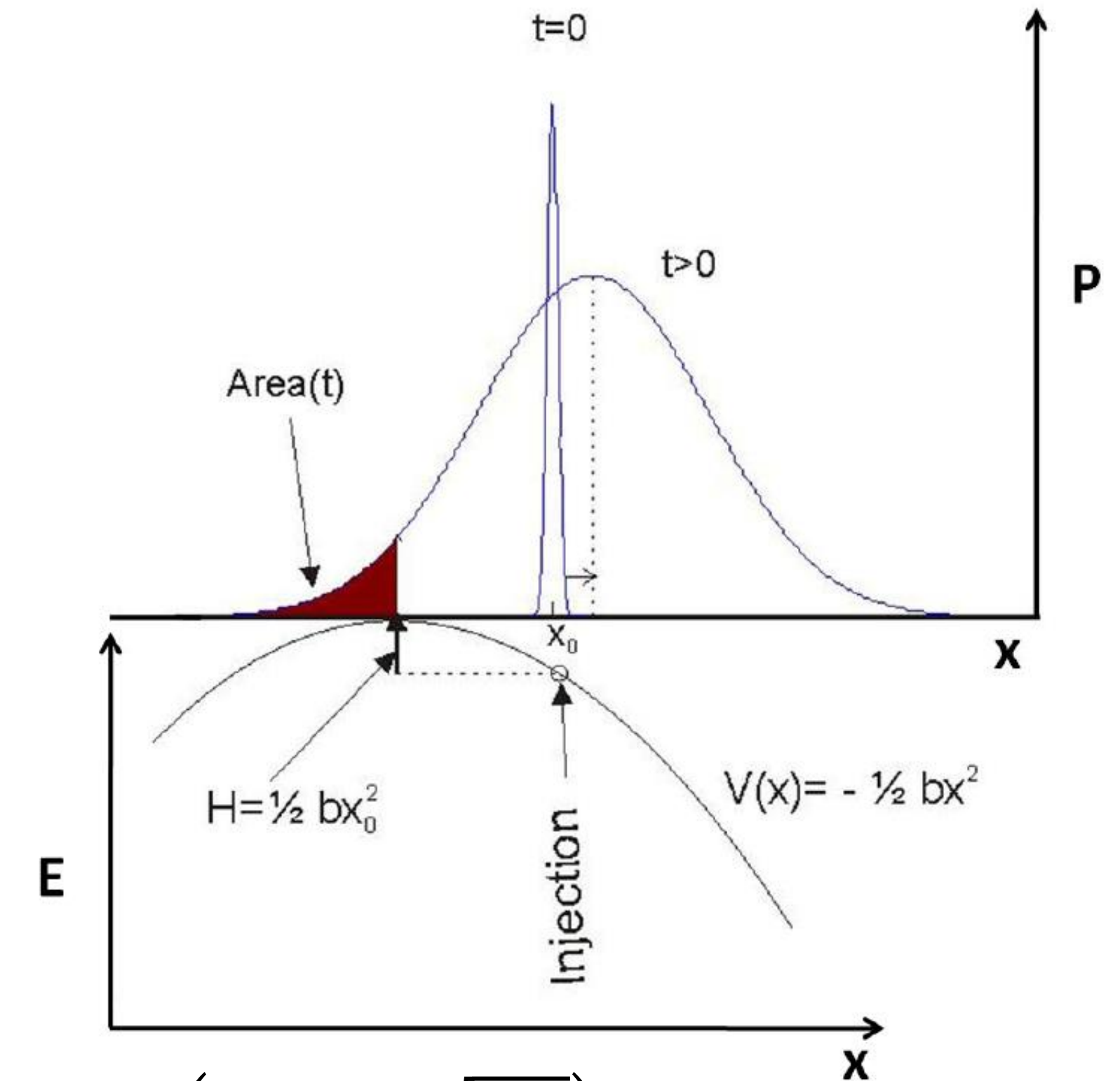
In the FBD model we use
1D motion approximation

The system must overcome an internal
barrier H to fuse.



L is the effective elongation (along the fusion path)

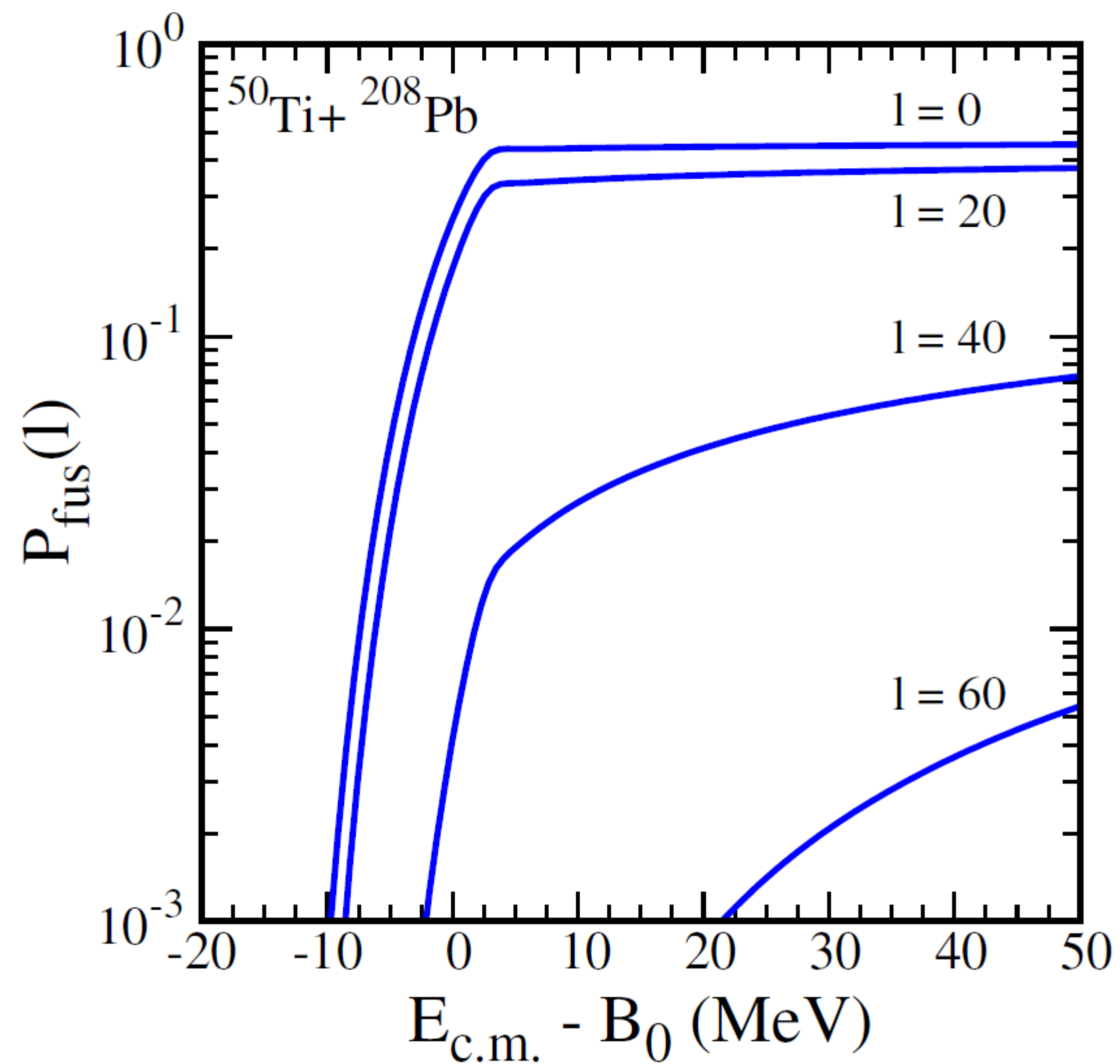
P_{fus} is calculated by solving
1D Smoluchowski Diffusion Equation



$$P_{fus}(l) = \frac{1}{2} \left(1 - \operatorname{erf} \sqrt{\frac{H(l)}{T}} \right) \text{ when } L_{inj} \geq L_{saddle}$$

$H(l)$ – the function of angular momentum
and bombarding energy

T – the temperature depends on available energy

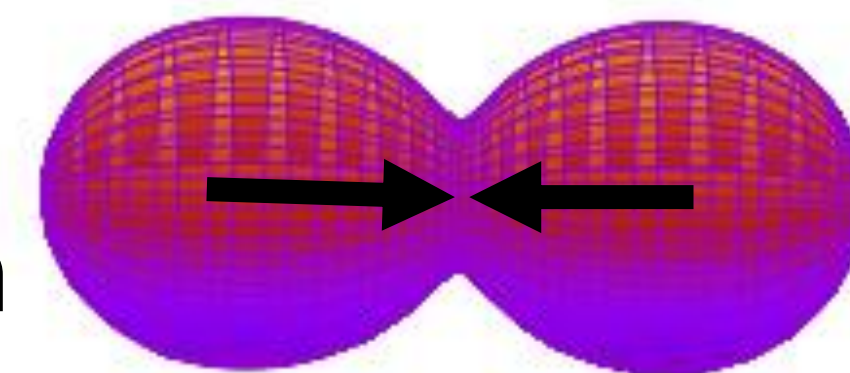


Available energy with respect to the entrance channel barrier B_0

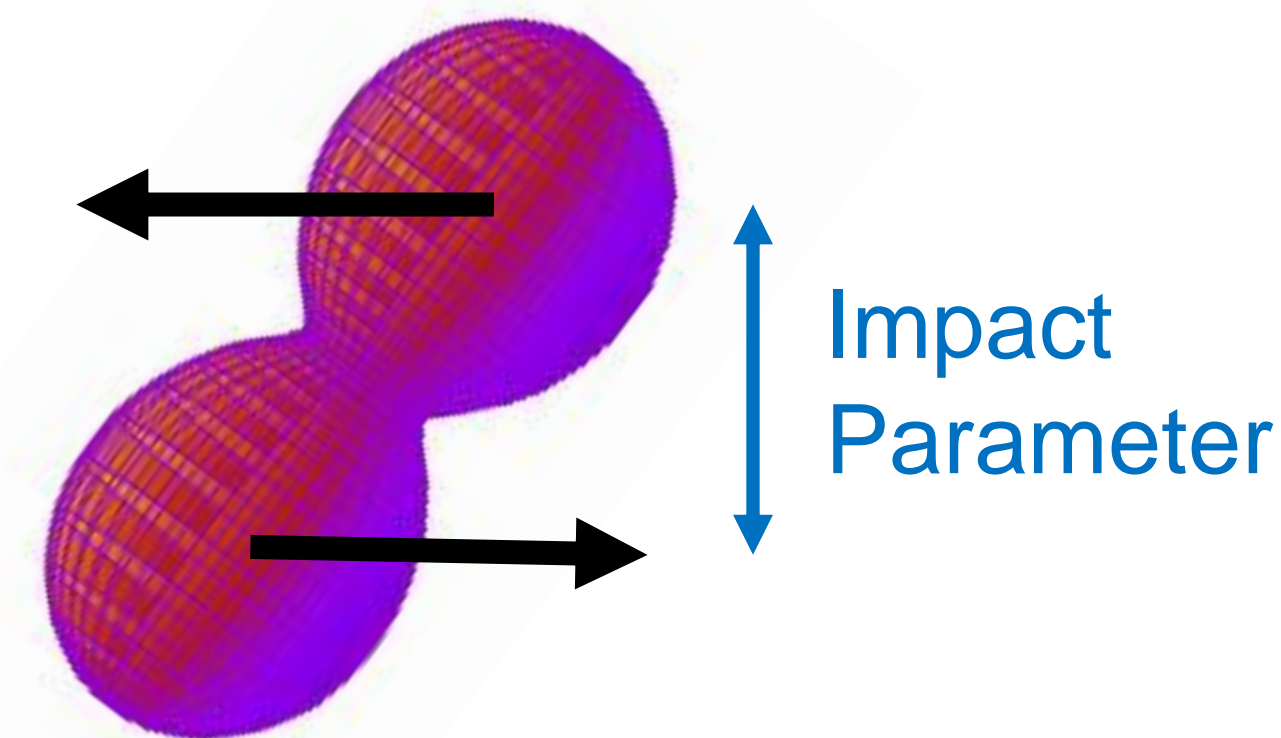
$$B_0 = 191.3 \text{ MeV}$$

$$E^*(E_{c.m.} = B_0) = 21.7 \text{ MeV}$$

$l = 0$
Central collision



Peripheral collisions



Higher partial waves l

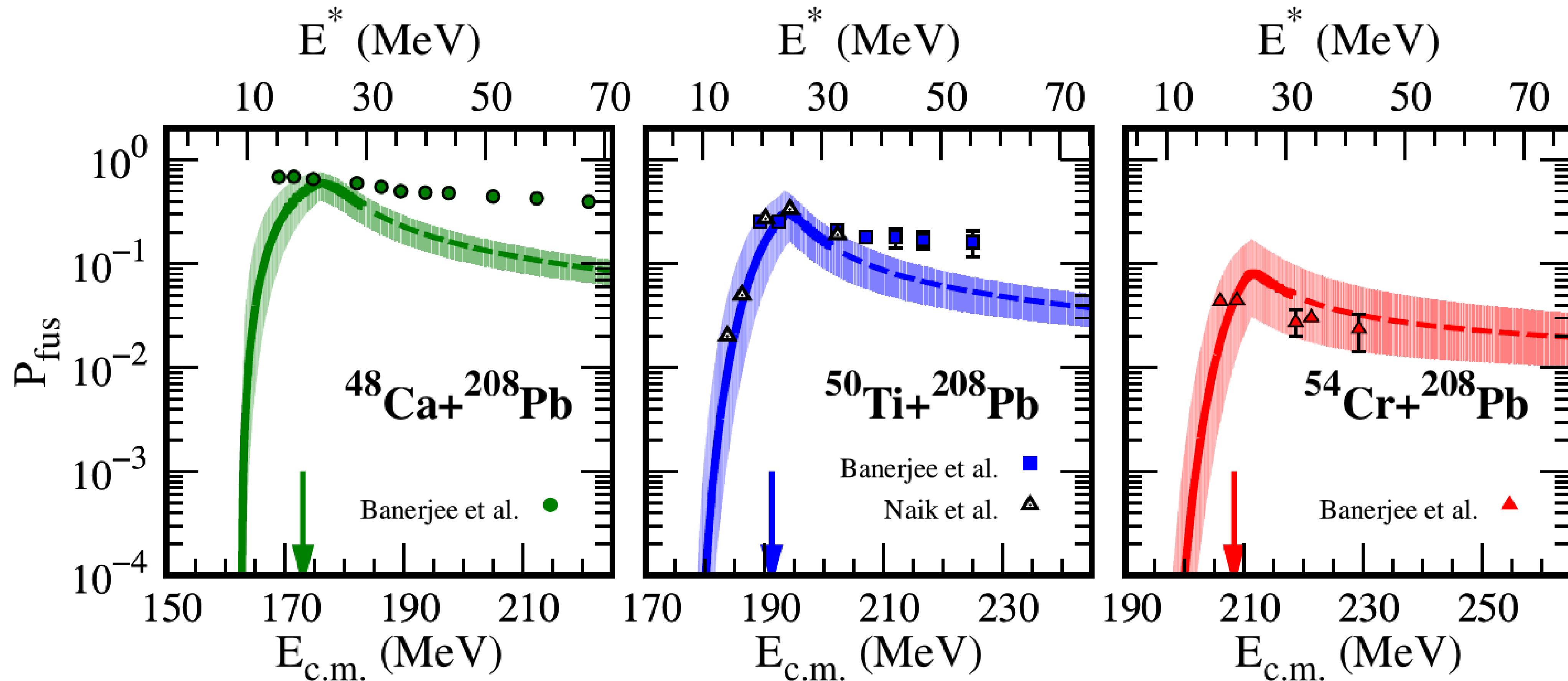
=

Higher rotational Energy

=

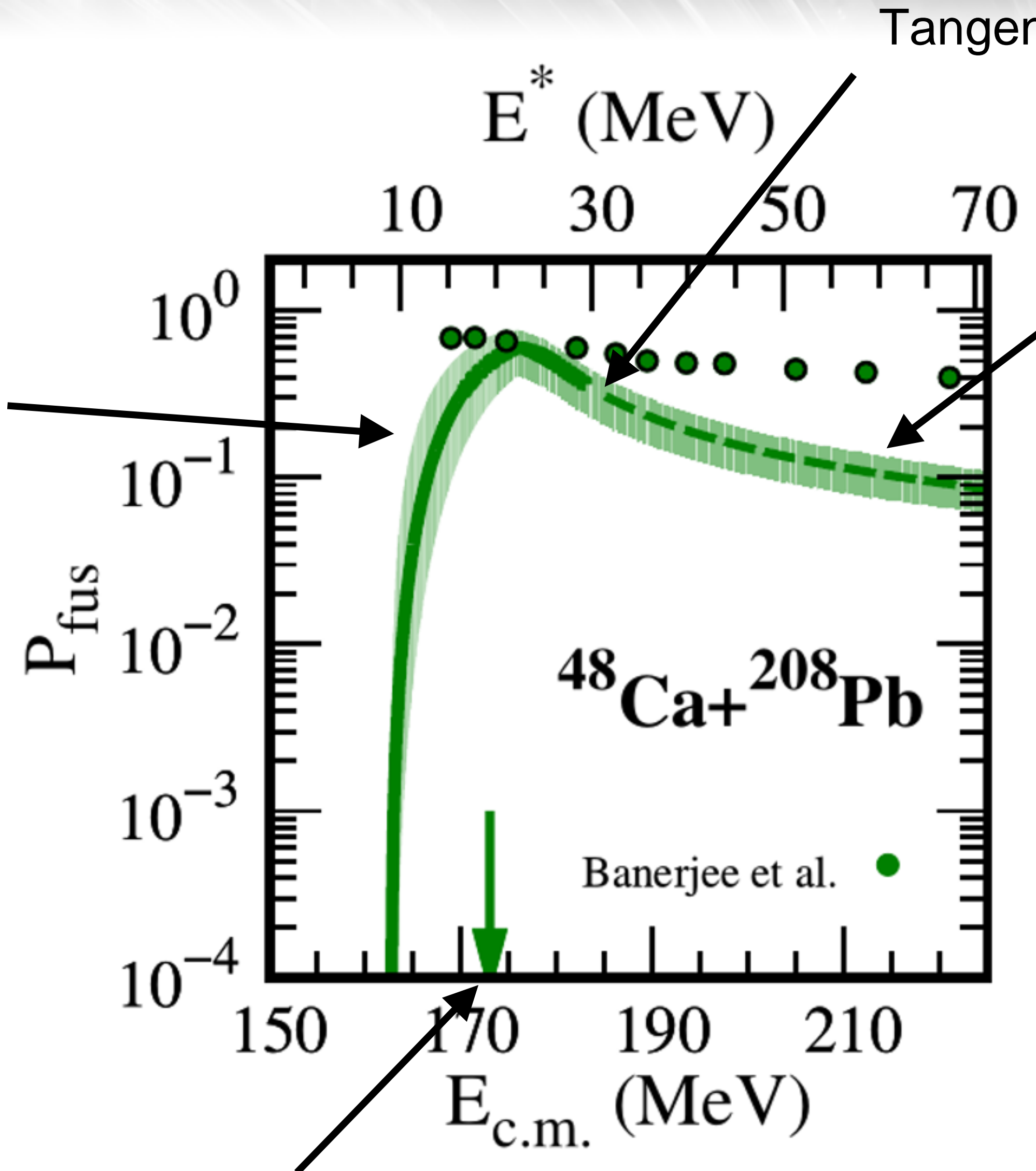
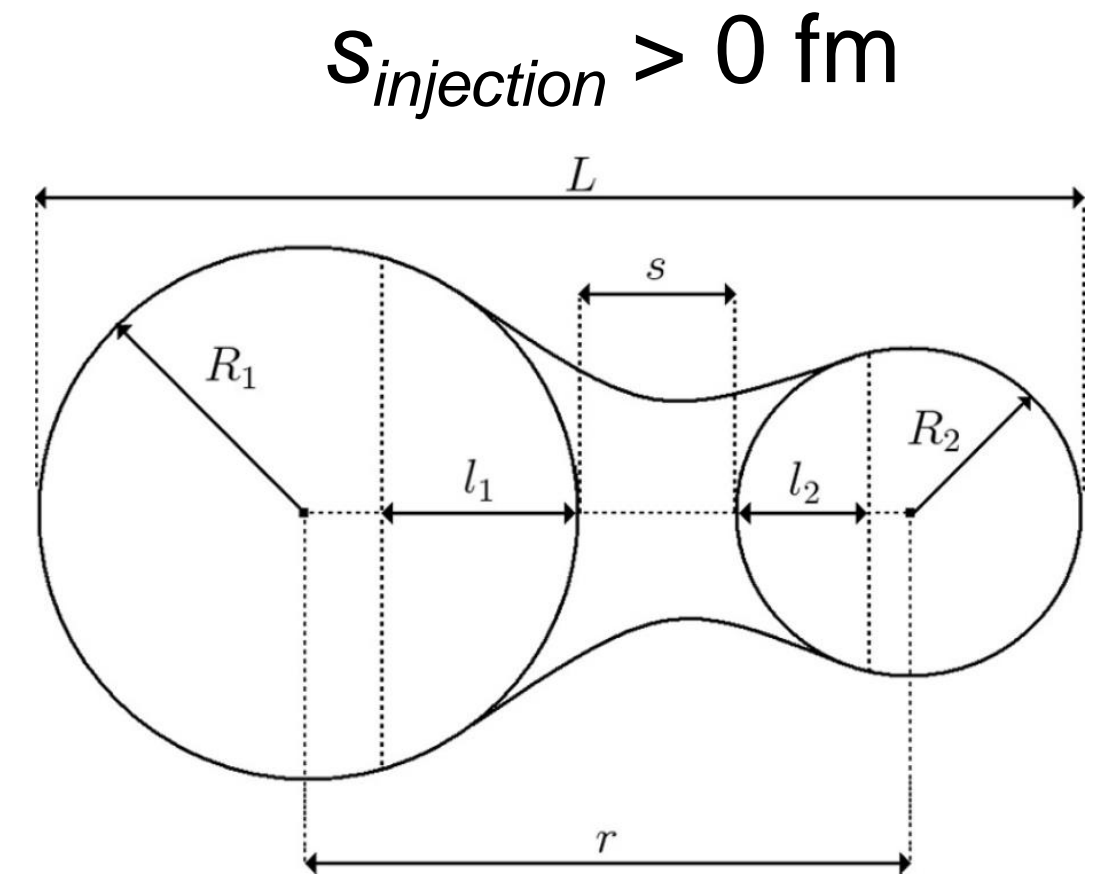
Lower P_{fus}

$$P_{fus}(E_{c.m.}) = \frac{\sum_{l=0}^{l_{max}} (2l+1) P_{fus}(l)}{(2l_{max}+1)^2} \quad \text{Fusion probability averaged over } l$$



Submitted to PLB, available at: [arXiv:2107.00579](https://arxiv.org/abs/2107.00579)

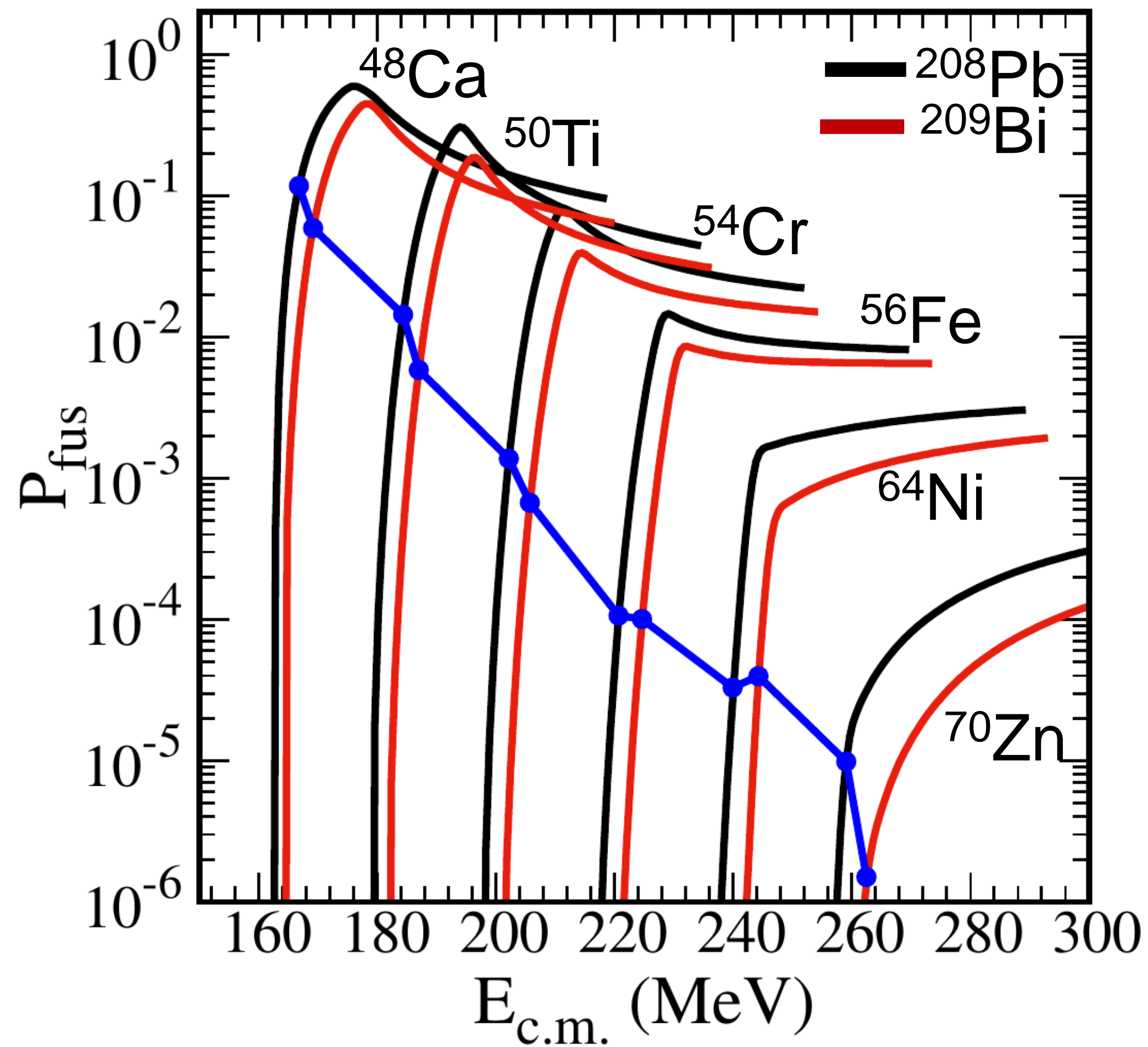
Below $B0$, the P_{fus} growth comes from the reduction in the height of the internal barrier opposing fusion.



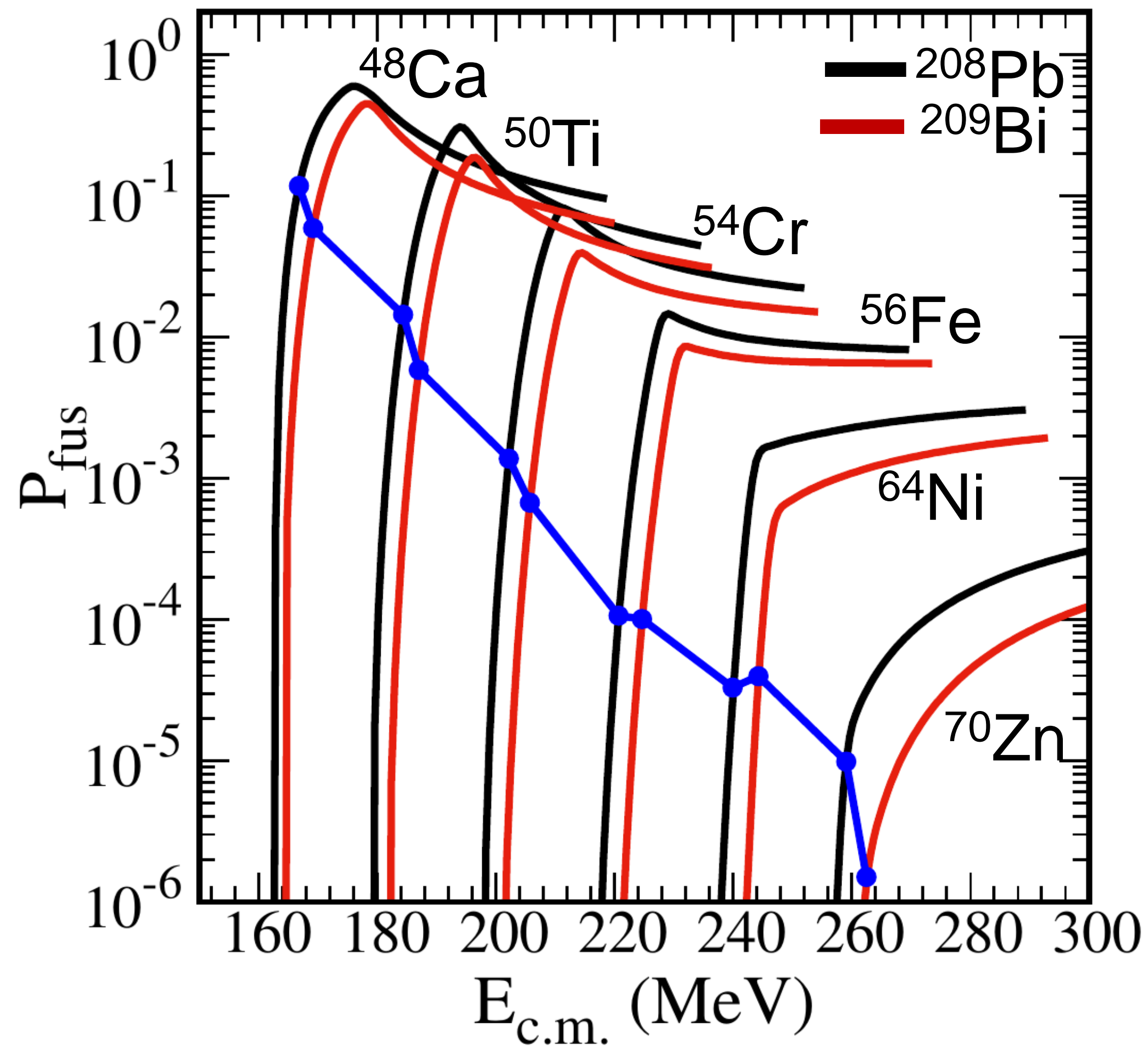
The P_{fus} saturation above $B0$ results from suppression of the contributions from higher partial waves and can be linked to the critical angular momentum.

The difference between rotational energies in the fusion saddle and the contact (sticking) configuration plays a major role in compound nucleus formation at energies above $B0$.

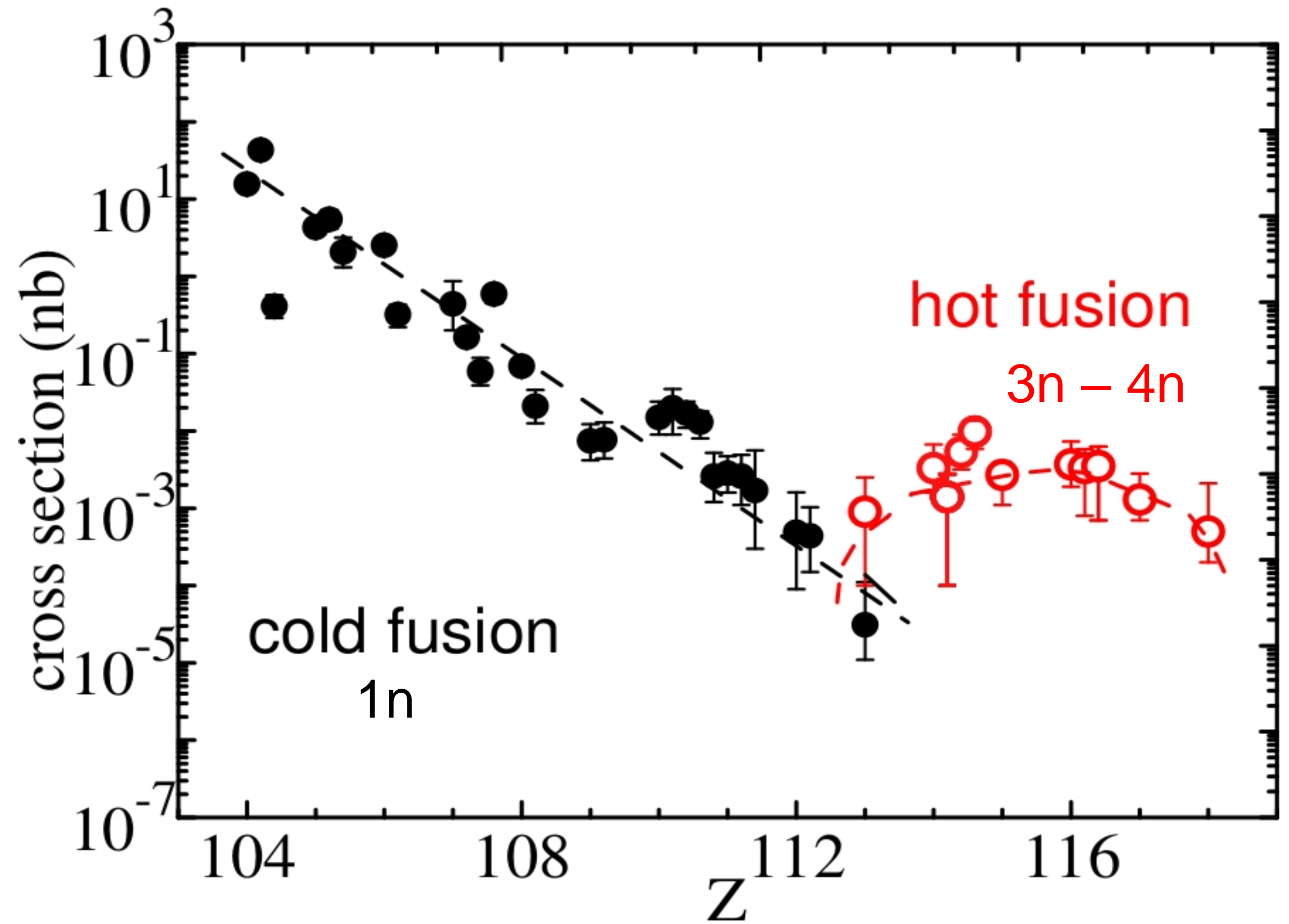
$B0$ - entrance channel barrier (Coulomb+Nuclear potential)



Blue line – Maxima of the 1n channel cross section for cold Fusion reactions



Blue line – Maxima of the 1n channel cross section for cold Fusion reactions



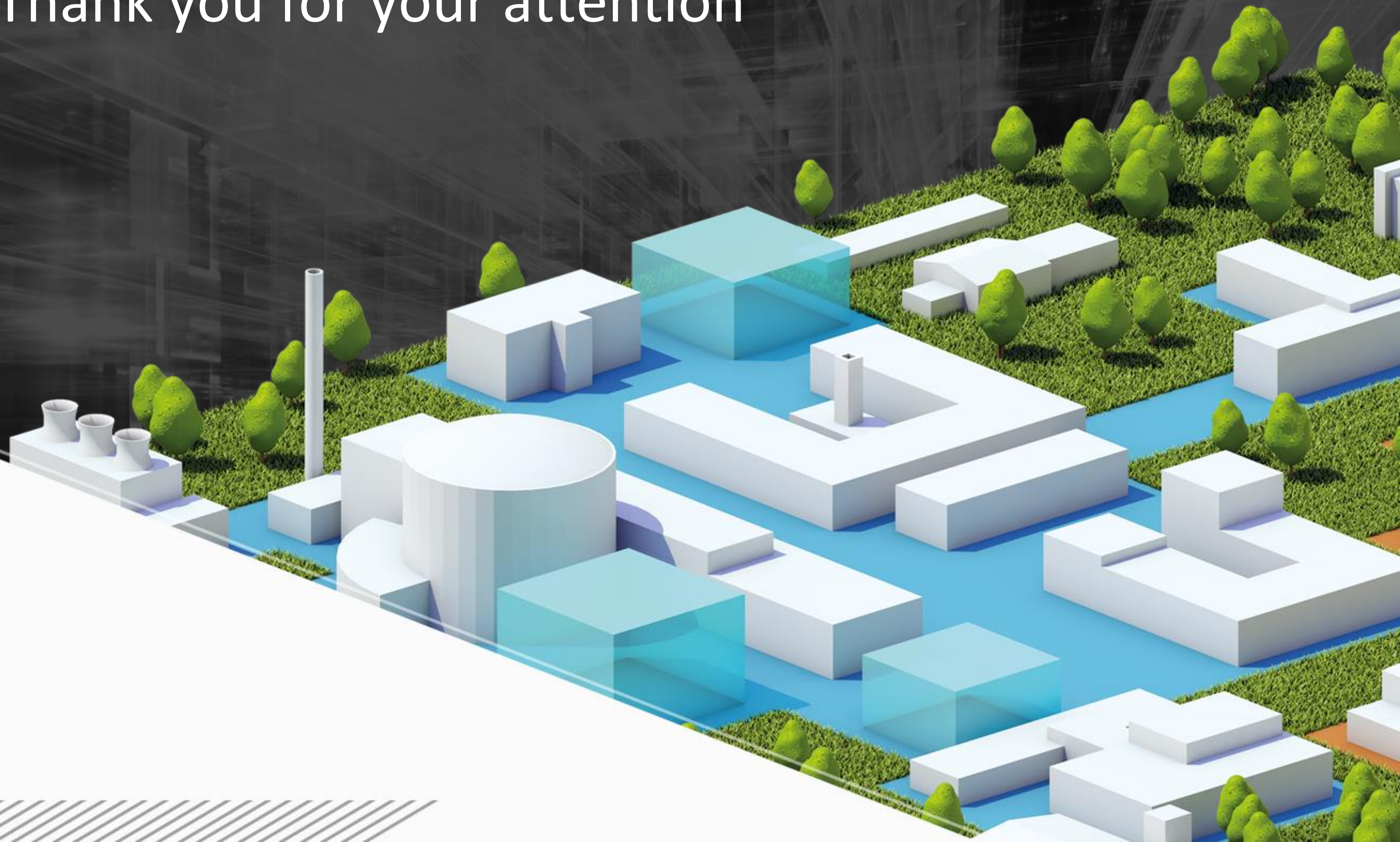
Next step – calculations for hot fusion reactions

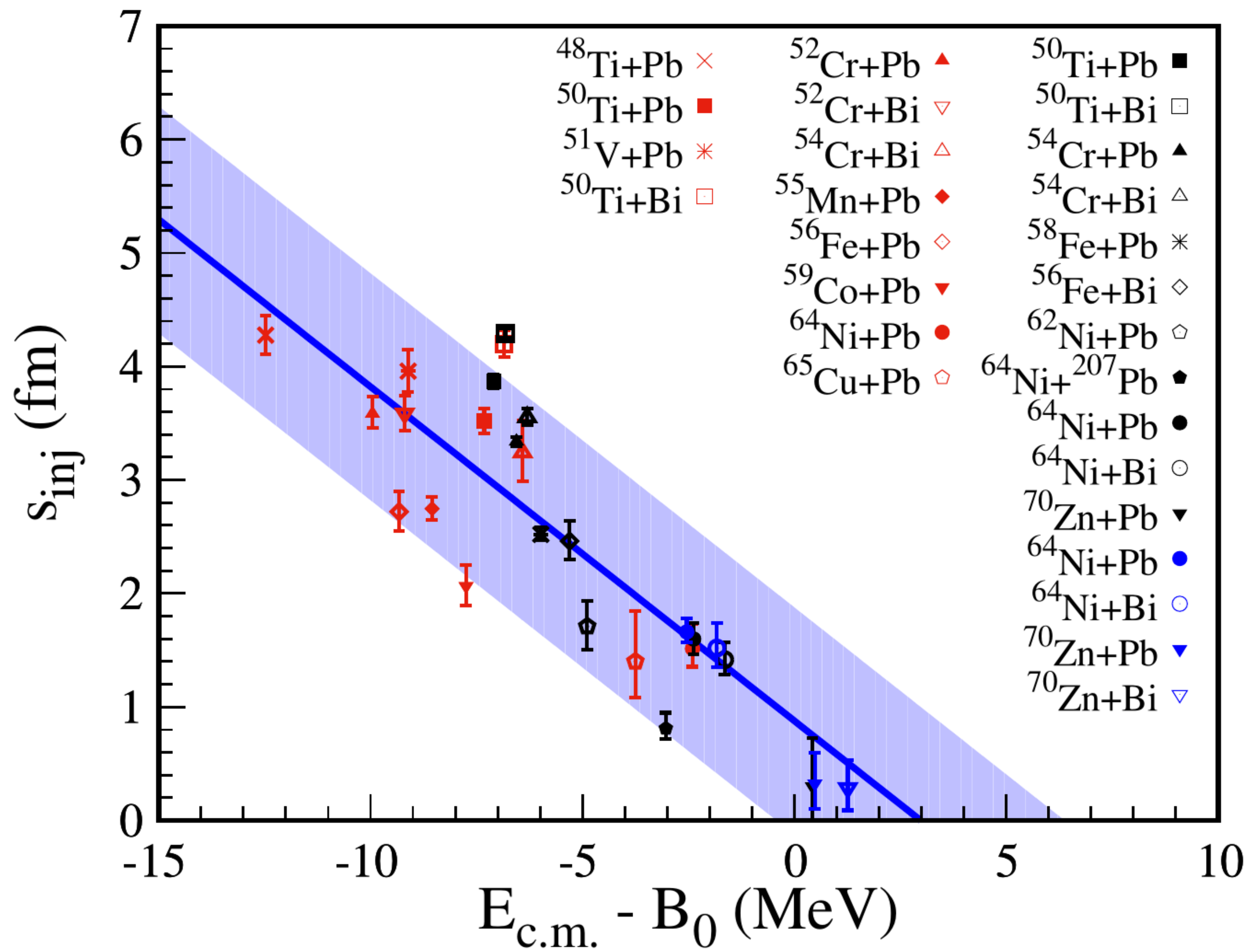
Thank you for your attention

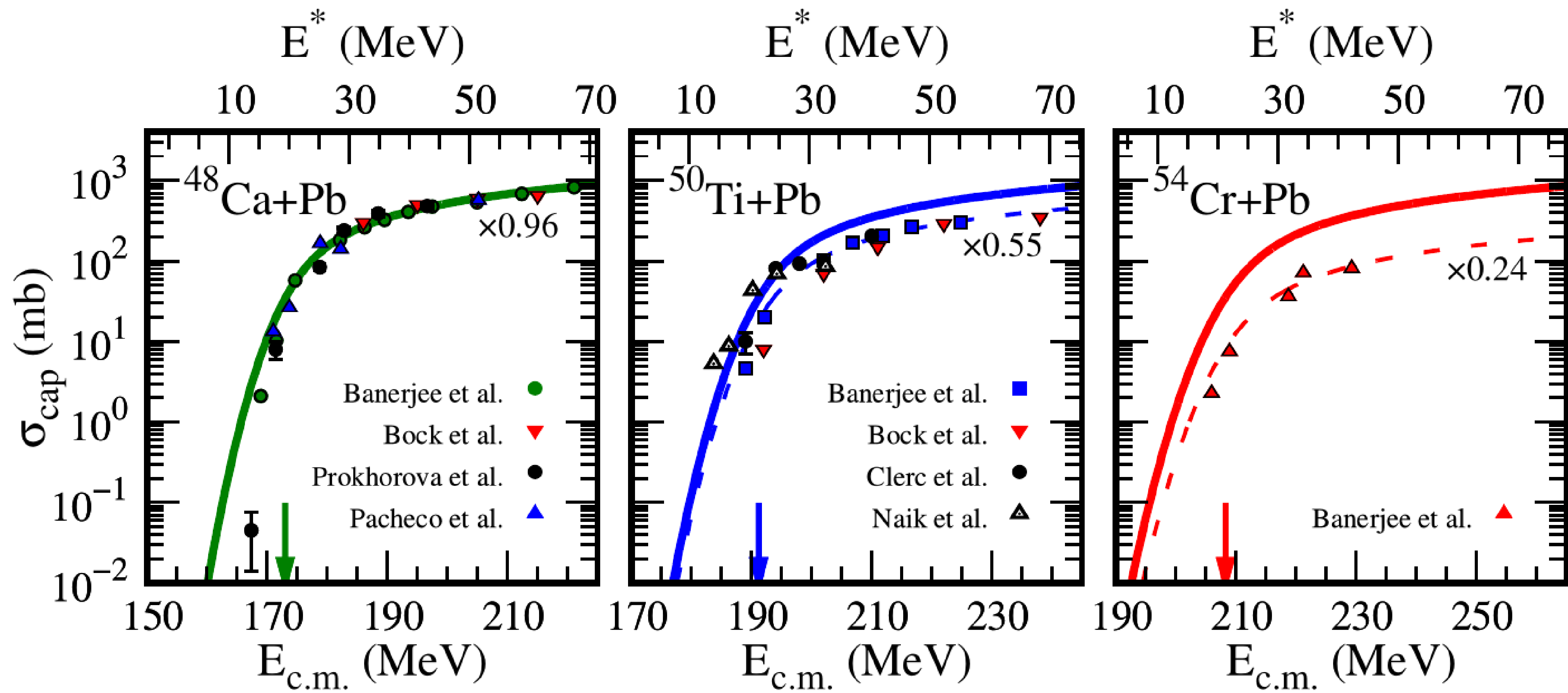


NATIONAL
CENTRE
FOR NUCLEAR
RESEARCH
ŚWIERK

www.ncbj.gov.pl







Smoluchowski Diffusion Equation

$$\gamma \frac{\partial W(x,t)}{\partial t} = -\frac{\partial}{\partial x} [bxW(x,t)] + T \frac{\partial^2}{\partial x^2} W(x,t)$$

\propto Viscosity of fluid

Driving force

Temperature

$W(x,t)$ = probability to find Brownian particle at position x at time t

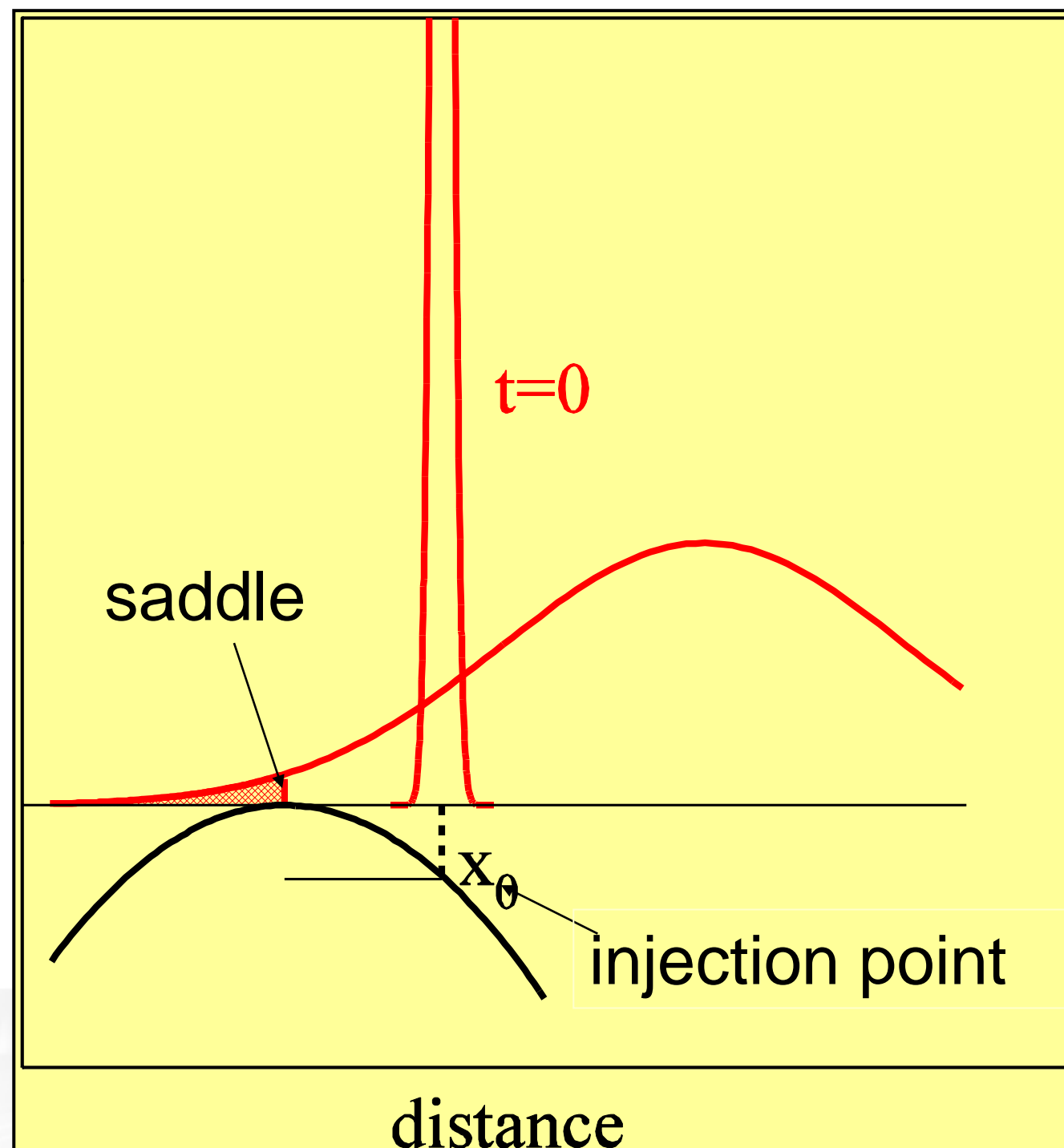
Exact solution in a parabolic potential
 $V(x) = -bx^2/2$ is a sliding, swelling Gaussian.

$P(\text{fusion})$ = fraction of Gaussian captured
 inside the barrier as $t \rightarrow \infty$

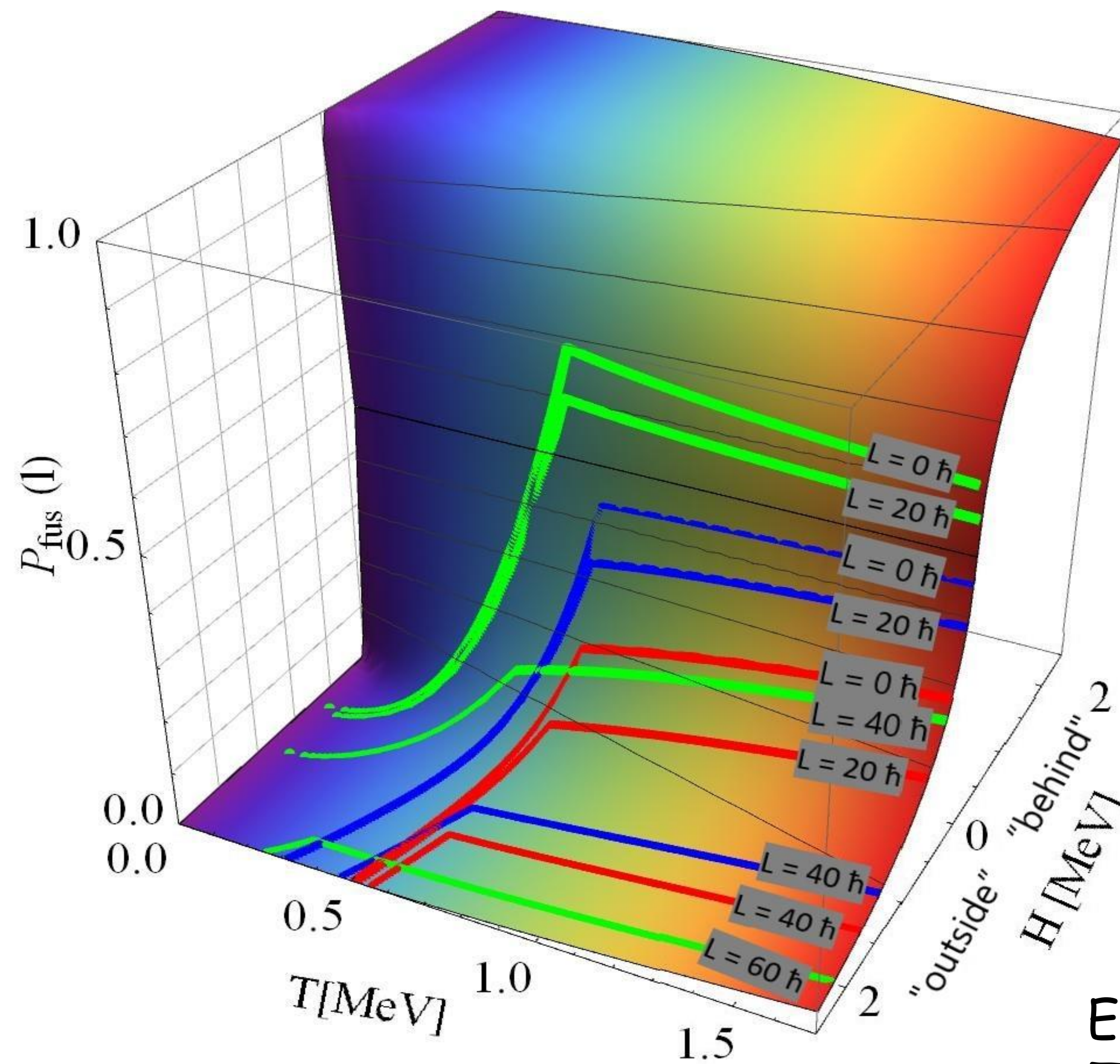
$$P(\text{fusion}) = \frac{1}{2}(1 - \text{erf}\sqrt{B/T}) \quad B = bx_0^2/2$$

if $x_0 \geq 0$ (injection point),

W.J. Świątecki, K. Siwek-Wilczyńska, J. Wilczyński
 Acta Phys. Pol. B34 (2003)2049, IJMP E13 (2004) 261,
 Phys.Rev.C71 (2005) 014602



^{48}Ca ^{50}Ti ^{54}Cr



$$E^* = aT^2$$

$$T = 1 \text{ MeV} \quad E^* \approx 30 \text{ MeV}$$